

A coupling of the origin of asteroid belt, planetary ring, and comet

Yongfeng Yang

Bureau of Water Resources of Shandong Province, Jinan, Shandong Province, China, Mailing
address: Shandong Water Resources Department, No. 127 Lishan Road, Jinan, Shandong Province,
China, 250014

Tel. and fax: +86-531-8697-4362

E-mail: roufengyang@gmail.com

Abstract

Observations show that there are an asteroid belt, four giant planetary ring systems, and countless comets in the solar system. Various scenarios in the past had been presented to account for their origins, but none of them is competent. Asteroid belt located between the orbits of Mars and Jupiter is flat, circular, and parallel to the ecliptic, similarly, planetary ring located between the orbits of satellites is also flat, circular, and approximately parallel to planetary equatorial plane. This resemblance implies that both asteroid belt and planetary ring are likely to derive from a common physical process. Here we propose 5 significantly disruptive collisions of the two bodies of binary planetary (satellite) systems in the history of the solar system to be responsible for the formation of asteroid belt and giant planets' ring systems. In each collision the two bodies of a binary system are firstly shattered into fragments and ejected towards all around, but due to the constraint of a hierarchical two-body gravitation (non-Newton's gravitation), the barycenter of initial binary system is survived in the collision, and the fragments are still organized in a series of hierarchical two-body systems. As inferred from Galileo's experiment of projectile, the fragments run some parabolic trajectories around the collisional origin, but at the same time the survived barycenter continues to orbit and drag the fragments to move by means of the barycenters of a series of two-body systems, by which nearby fragments are confined to gradually fall on a circular belt (ring). Some of the falling fragments are further shattered into very small fragments to form

independent belts (rings). The collision of the two bodies of a binary planetary system gives birth to asteroid belt, while the collision between the two bodies of a binary satellite system gives birth to a planetary ring system. Further fragments (relative to the collisional origin) in travel bombard the objects they encounter and leave craters on the surfaces. Due to the motions of the survived barycenter around the Sun (giant planet) and giant planet around the Sun, these further fragments are being brought to run through the solar system back and forth, this results in the advent of comets when close enough to the Sun (if they hold icy materials), and appearance of meteors when close enough to the Earth, some of the fragments occasionally landed on the surfaces of planets and satellites and become meteorites.

1 Background

Long-term ground and spacecraft-based observations confirm that there are an asteroid belt, four giant planetary ring systems, and countless comets in the solar system. The origin theories of planetary ring are plentiful. Especially for the Saturn's ring, they include tidal disruption of a small moon (Roche et al. 1847), unaccreted remnants from the satellite-formation era (Pollack et al. 1976), disruptive collision of a small moon (Charnoz et al. 2009), and tidal disruption of a comet (Dones 1991). Canup (2010) concluded the disabilities of these theories and developed a model of planetary tidal force stripping ice material from a Titan-sized satellite. The previous origin theory of asteroid belt thinks that asteroids are fragments of a destroyed planet (Herschel 1807), the currently accepted scenario believes asteroids to be the rocks that in primordial solar nebula never accumulate into a genuine planet (Petit et al. 2001). The origin theory of comet mainly includes Oort cloud hypothesis that proposes a cloud of comets at the outer reaches of the solar system (Oort 1950) and Kuiper belt hypothesis that proposes a disc shaped region of space outside the orbit of Neptune to act as a source for short-period comets (Kuiper 1951). However, a large number of observations are strongly questioning these plausible scenarios. If the Saturn's rings are from a previous pure ice ring as Canup proposed (2010), it is necessary for them to hold identical material, but observation shows that there are various spectral characteristics (corresponding to different materials) in the Saturn's rings, moreover, different spectral rings around the planet are parallel to each other, any general mechanism is very difficult to create such a strange distribution. To support the production of icy moons, Canup employed another work by Charnoz et al (2010)

that ring material spreading beyond the Roche limit may accrete to form icy moons. But the Roche limit itself is doubtful because a lot of satellites whose distances from their father planets (Jupiter, Uranus, and Neptune, for example) are interior to the Roche limit are still existed (Burns et al. 2001). The Saturn's rings are broad and separated by many divisions that look like natural boundaries, particles in each ring appear to be very orderly and never ride over these boundaries. This orderliness requires a longitudinal confinement mechanism to be responsible for. We also see a big difficulty in understanding the dynamics of the Uranus's narrow rings and Neptune's ring arcs. The Uranus possess more than 13 narrow rings, within them a number of clump structures are distributed, this needs some kind of mechanism to hold these structures together. Goldreich and Tremaine proposed a series of small satellites exerting gravitational torques to confine the Uranus' rings (1979). To be effective, the masses of the satellites need to exceed the mass of the ring by at least a factor of two to three (Porco et al. 1987). But only the ϵ ring is so far observed to have two small companions - Cordelia and Ophelia, no satellite larger than 10 km in diameter is known in the vicinity of other rings (Smith et al. 1986). The Neptune's ring arcs currently keep unresolved (Miner et al. 2007), even though a large number of models (Smith et al. 1989; Salo and Hnninen 1998; Dumas et al. 1999; Sicardy et al. 1999; Namouni and Porco 2002; Renner and Sicardy 2003 and 2004) in the past 20 years had been attempted.

Herschel's idea of forming asteroid belt (1807) was rejected due to its disability in explaining the supply of shattering energy and the diversity of asteroids' composition. The currently accepted model proposed by Petit et al (2001) is that the asteroids are the planetesimals that were left from primordial solar nebula. This thought, however, is strongly against an observational fact. It is already confirmed that a large body of asteroids in the belt belong to some families (or groups), in which these asteroids share not only similar chemical composition but also similar orbital elements such as semi-major axis, eccentricity, and orbital inclination. If the asteroids were the planetesimals of primordial solar nebula, any random movement between the planetesimals will not allow those who hold similar chemical composition to cluster into a physical association. So far, around one-third of the asteroids in asteroid belt have been confirmed to be the members of an asteroid family. Given the limitation of observation, we still have chance to classify more asteroids into some families. Most importantly, the nebula hypothesis itself is being seriously surrounded by a series of problems such as the loss of angular momentum, the disappearance of

the disk, the formation of planetesimals, the formation of giant planets and their migration, and so on (Woolfson 1993; Taishi et al. 1994; Andrew et al. 2002; Klahr and Bodenheimer 2003; Inaha et al. 2003; Wurchterl 2004), the planetesimal therefore is nothing but a hypothesis of hypothesis. The two origin theories of comet are also questionable. Jan Oort (1950) statistically found that there is a strong tendency for aphelia of long period comet orbits to lie at a distance of about 50,000 AU and then concluded that comets reside in a vast cloud at the outer reaches of the solar system. It is important to note that this so-called aphelia of comet orbit is derived from a Keplerian expectation other than observation, nobody in person sees that the end of a comet's orbit is located at such a distant place. In practice, when we observe a comet, the Earth is rotating around its axis, at the same time the Earth-Moon system is also rotating around the common center of their mass, and this barycenter is also revolving around the Sun, what we see is a compositive impression for the comet. In other words, it is rather difficult to know a comet's proper motion. In addition to this, the solar system in appearance is flat, it seems no reason to support the existence of a spherical cloud of comets. On the other hand, the orbital features of short period comets do not approve an origination from Oort cloud, and the mechanism by which the comets are supplied from Kuiper belt to planet-crossing orbits is still unknown (Duncan et al. 1988). In the last 20 years, though a lot of Trans-Neptunian objects had been found from the proposed Kuiper belt, there is no evidence to show that these objects are indeed linked to comets. The recent discovery of main belt comets (Hsieh et al. 2006) further indicates that the origin of comet is likely to be different from the expectation of conventional knowledge.

In conclusion, these established origin theories of asteroid belt, planetary ring, and comet are so questionable that we need to run a comprehensive consideration. Both asteroid belt and planetary ring are flat, circular, and parallel to respectively the ecliptic and planetary equatorial plane; they are embedded respectively in the planetary orbits and in the satellites' orbits; In addition to this, asteroids consist primarily of carbonaceous, silicate, and metallic materials, which is similar to the chemical composition of the Earth and Mars. Relatively, planetary ring consists primarily of ice and dust, which is similar to the chemical composition of icy satellites. On large scale, the Sun has a lot of planets, giant planet (Jupiter, Saturn, Uranus, and Neptune) also has a lot of satellites. This similarity suggests that asteroid belt and planetary ring are likely to share a common forming mechanism. On the other hand, the Saturnian F ring and the Uranian ϵ ring are

narrow, and are often shepherded by a pair of moons (Esposito 2002), the outer rings of Uranus are similar to the outer G and E rings of Saturn (Pater et al. 2006), narrow ringlets in the Saturnian rings also resemble the narrow rings of Uranus, the Neptunian ring system is quite similar to that of Uranus (Esposito 2002; Burns et al. 2001). This similarity suggests that four giant planets' ring systems are likely to be ruled by a common physics. The observations of crater, star, exoplanet, and satellite also offer significant suggestion. The craters on the surfaces of planets and satellites indicate that there had taken place some great bombardment events in the history of the solar system. The analysis of impact crater record confirms an inner solar system impact cataclysm occurred 3.9 Gy ago (Strom et al. 2005), while the heavily crater surfaces on Ganymede and Callisto confirms other impact cataclysms occurred in the outer solar system (Strom et al. 1981). These impact cataclysms require different projectile origin at different time to be responsible for. A number of observations confirm a fact that the orbit of celestial object is generally decreasing. The two stars in binary star system RX J0806.3+1527 are steadily decreasing orbital period at a rate of 1.2 milliseconds per year. The orbital period of binary star Cen X-3 and SMC X-1 is decreasing at a rate of respectively $P_{orb}/P_{orb} = 1.8 \times 10^{-6} \text{ yr}^{-1}$ and $3.36 \times 10^{-6} \text{ yr}^{-1}$ (Kelley et al. 1983; Levine et al. 1993). PSR B1913+16 have a rate of decreasing orbital period of 76.5 microseconds per year, and the rate of decrease of semimajor axis is 3.5 meters per year (Weisberg and Taylor 2004). Many hot giant planets are detected to be revolving around stars with very short-period orbits. The members of "51 Peg" planets, 51 Peg itself, Tau Bootis, 55 Cancri, and Upsilon Andromedae, have orbital periods of just 4.2, 3.3, 14.7, and 4.6 days, respectively, and their orbits are very small, with radii less than 0.11 AU. A steamy planet is recently found to be orbiting a faint star with a distance of just 1.3 million miles (Terquem and Papaloizou 2007). This short-period orbit suggests that these extrasolar planets could have been giant icy planets formed far enough from their stars that ices could condense, and then have migrated towards their stars (Brunini and Cionco 2005; Raymond et al. 2008; Charbonneau et al. 2009). The moon of Mars, Phobos has a decreasing orbit at a rate of 1.8 cm/yr (Clark 2010). So far, there is very little evidence to show that the orbit of celestial object is increasing, especially for planet and satellite, and because the effect of gravitation is to drag objects to approach each other, we therefore infer that the orbital decrease of celestial object is necessary, even though it is very difficult to be found in the solar system. A decreasing orbit destined an increase in orbital velocity and a catastrophic

collision between the two bodies. In addition to these, the well-regulated movement of asteroid family (group) (Hirayama 1918), the integrity of the Saturn's narrow F ring (Murray et al. 2008), and the twisted arc in the Neptune's Adams ring (Hammel 2006) appear to indicate that they do not obey a constraint of Newton's gravity. Yang (2011) recently introduced a model to show that all objects in the universe are initially built up from small units (ordinary particles) through a pattern of one-capture-one and therefore organized in a series of hierarchical two-body systems to orbit, and that the two bodies of a two-body system due to orbital decrease will eventually take place a collision. A natural result from the collision of two bodies is to shatter them into small fragments, these fragments may further bombard the objects they encounter in travel, but under the effect of hierarchical two-body gravitation they may be confined to fall on a circular belt. Some of them, if hold volatile material and close to the Sun, may become comets. In this present paper, we totally formulate 5 physical collisional scenarios of the two bodies of binary planetary (satellite) system to clear up all suspicions above at the same time and further account for some observations.

2 Modelling

A recent work by Yang (2011) proposed that every celestial object was initially built up from small units (particles) by means of a pattern of hierarchical two-body capture. This means that if a celestial object is shattered into fragments, these fragments are still gravitationally constrained in a series of hierarchical two-body systems and the barycenter of initial celestial object may be survived in the disruption. Based on this deduction, a conceptual model is developed to formulate the formation of a belt (ring) (Fig.1): a two-body system is orbiting around a center body; with the passage of time, the two bodies of the two-body system due to orbital decrease take place a smashing collision and are shattered into fragments. But due to the constraint of a hierarchical two-body gravitation, the barycenter of initial two-body system is survived in the collision, and the fragments ejected are still organized in a series of hierarchical two-body systems; The barycenter continues to orbit and drag these fragments to move by means of the barycenters of a series of hierarchical two-body systems, by which nearby fragments are confined to gradually fall on a circular belt (ring). As shown in Figure 1(D), the barycenter of initial two-body system (point O) is dragging two components (point a and 1) to orbit, at the same time point a is also dragging two components (point b and d) to orbit, point b is also dragging two components (point c and one

fragment) to orbit, etc. Because of this successive hierarchical drag from point O and related points to these fragments, they can always obtain some motions to longitudinally spread out. With the passage of time, they will have to fall on a circular belt (ring) around the center body. Because of orbital decrease, the barycenter of initial two-body system continues to drag all fragments to immigrate towards the center body, the differential motion between these fragments will lead them to radially spread out, the belt (ring) slowly becomes wide.

I here formulate one collision of binary planetary system and four collisions of binary satellite system in the history of the solar system. For the collision of binary planetary system, the center body is replaced with the Sun, the composition and mass of binary planetary system are similar to that of the Earth-Moon system, and it is located between the orbits of the Mars and Jupiter. The collision occurred at the time of around Late Heavy Bombardment. After the disruption of the two bodies, countless fragments are randomly ejected towards all around. Due to a successive hierarchical two-body drag, nearby fragments are confined to gradually fall on a circular belt, while further fragments (with respect to the collisional origin), because of the motion of the survived barycenter around the Sun, are brought to run across the solar system back and forth. Water in the disruption is sealed into the bodies of some fragments, while atmosphere is either escaped or sealed in the bodies of some fragments. This collision mainly gives birth to asteroid belt. For the four collisions of binary satellite system, the center body is replaced with Jupiter, Saturn, Uranus, and Neptune, respectively, the composition and mass of binary satellite system is similar to that of icy satellite of giant planet, and the binary satellite system is located between the orbits of planet and its major satellite. The four collisions of binary satellite system occurred generally later than the time of Late Heavy Bombardment. After the disruption of the two bodies, fragments are ejected towards all around. Due to a successive hierarchical two-body drag, nearby fragments are confined to gradually fall on a circular belt, and some of these falling fragments are further shattered into very small fragments (particles with a size of meter or micron, for instance) that are still constrained in a series of hierarchical two-body systems, and thereby form small independent rings, while further fragments (with respect to the collisional origin), because of the motion of the survived barycenter around the planet and the planet around the Sun, are brought to run across the solar system back and forth. These four collisions mainly give birth to giant planet's ring systems.

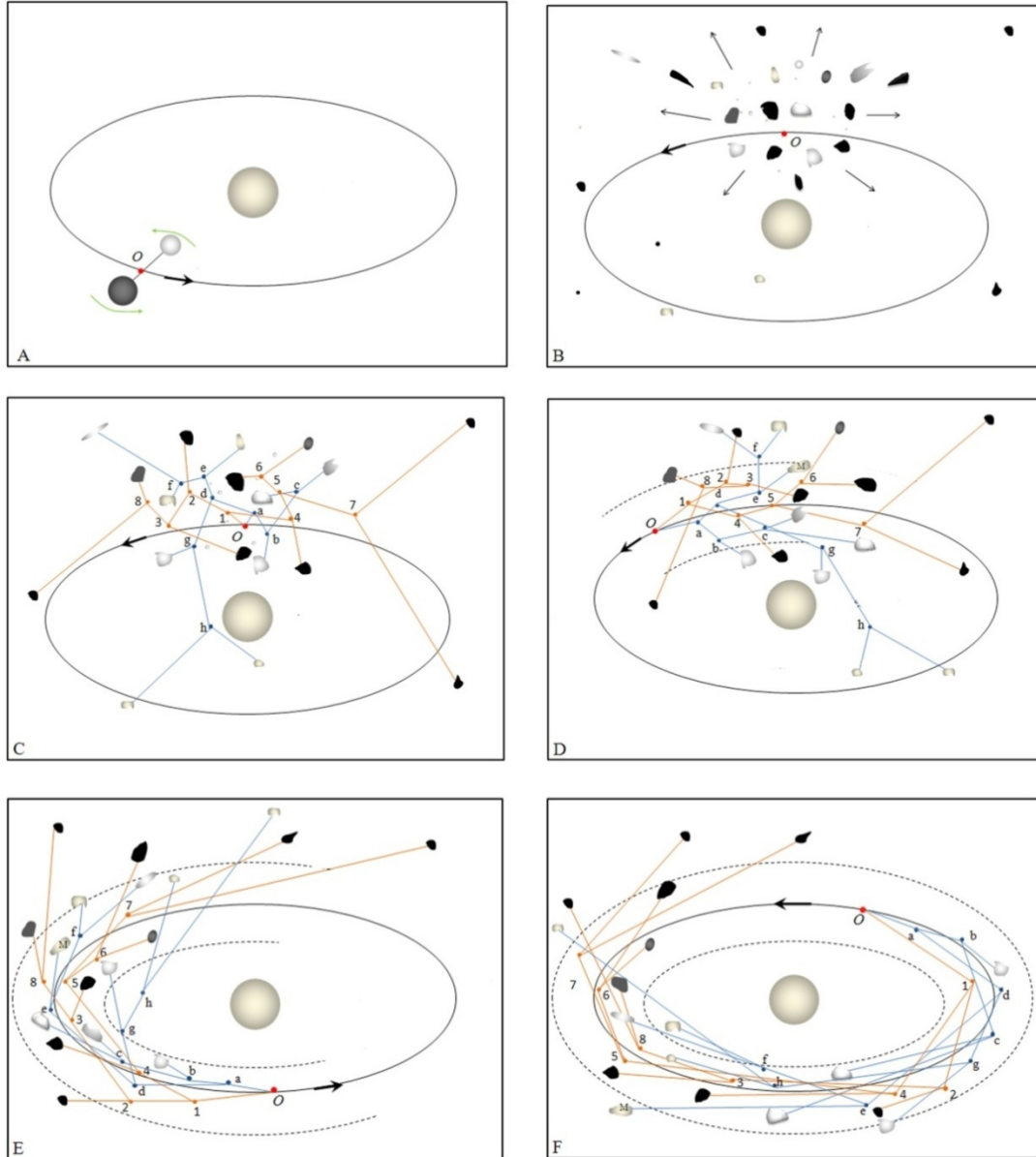


Figure 1: Simulation of the formation of a belt (ring system) based on hierarchical two-body gravitation. From A, B, C, D, E to F, it demonstrates the formation of a belt (ring system). Point O (marked with red dot) denotes the barycenter of initial two-body system. Blue (orange) dots (marked with letter a, b, c , etc., and number 1, 2, 3, etc.) represent the barycenters of related two-body systems. Blue (orange) line represents gravitation. Large black arrow represents the motion of the integral association. Dashed circle denotes the boundary of the belt (ring system). Note that these fragments are dragged by the center body's gravitation to orbit by means of the barycenter of the initial two-body system (point O) and the barycenters of a series of subordinate two-body systems (letter a, b, c , etc., and number 1, 2, 3, etc.).

3 Match with observation

3.1 Asteroid belt

Long-term observation shows that a large number of irregularly shaped bodies are occupying a wider region that is located approximately between the orbits of the Mars and Jupiter. The majority of these bodies are clustered in a belt of around 2.15 to 3.3 AU from the Sun. Over 200 known asteroids in the belt are larger than 100 km (Tedesco and Desert 2002). Data from Minor Planets Center shows that a population of 700 000 ~ 1.7 million asteroids are with a diameter of 1 km or more. The belt is proved to be composed primarily of three categories of asteroids: C-type or carbonaceous asteroids, S-type or silicate asteroids, and M-type or metallic asteroids, and that approximately one-third of the asteroids in the belt belong to some families (or groups), in which they share similar chemical composition and orbital elements, such as semimajor axis, eccentricity, and orbital inclination. Three bands of dust within the main belt have also been found to share similar orbital inclinations as the Eos, Koronis, and Themis asteroid families (Love et al. 1992). Data from Minor planets Center also shows that most asteroids within asteroid belt have large orbital eccentricities and various orbital inclinations.

Reference to Figure 1, it can be inferred that the fragments rejected from the disruption of the two bodies of binary planetary system must be irregularly shaped, and that under a hierarchical two-body confinement these fragments will be dragged to gradually fall on a circular belt around the Sun. A natural result from the disruptive collision is the majority of the fragments must be small in size. The composition of binary planetary system is similar to that of the Earth-Moon system, this determines fragments ejected to be composed of mainly C-type or carbonaceous, S-type or silicate, and M-type or metallic materials. It can also be inferred that some of these fragments may be further shattered into smaller fragments that are still organized in a series of hierarchical two-body systems, and the disruption of a fragment may form a physical association of smaller fragments that may be called a family (or group). As every fragment is dragged by a barycenter to orbit, and at the same time the barycenter is dragged by the barycenter of a superior two-body system to orbit, this determines that the fragments in a family (or group) must share identical orbital elements such as eccentricity, period, and inclination. Also because the fragments in a family (or group) are derived from the disruption of a common parent body, this determines them to hold identical composition. After the disruption of the two bodies, the melting materials

may be released and recrystallized due to a change of temperature and pressure. The asteroids are observed to generally hold irregularly smooth appearances, this may be explained as the sharp (asteroids) fragments had been long-termed erode by interstellar dust. Figure 2 shows an artistic configuration of asteroid belt, in which all asteroids are being organized in a series of hierarchical two-body systems to orbit. The asteroids are dragged mainly by the Sun's gravitation by means of the barycenter of the initial binary planetary system (point O) and the barycenters of a series of subordinate hierarchical two-body systems. Also note that the movement of each asteroid (or asteroid family) is a consequence of the interaction of inertia and gravitation, in which the inertia keeps the asteroid (or asteroid family) to move in a straight line, but the gravitation forever drags the asteroid (or asteroid family) to deviate from the straight line, a curving motion for the asteroid (or asteroid family) is thus determined.

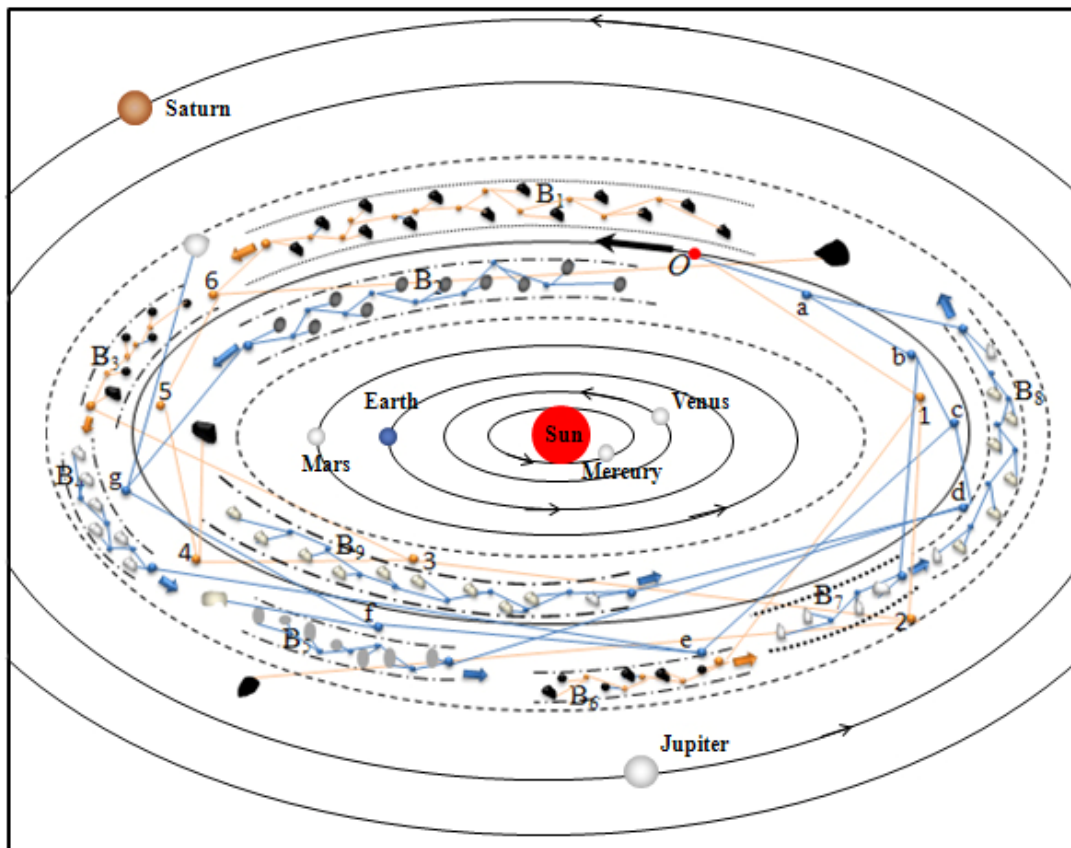


Figure 2: Configuration of asteroid belt. Different color in the asteroid's body denotes holding different composition. Point O (marked with red dot) denotes the barycenter of asteroid belt. B_1, B_2, B_3 etc. denote asteroid families that consist of a series of subordinate hierarchical two-body systems of smaller asteroids. Blue (orange) dots (marked with letter a, b, c , etc., and number 1, 2, 3, etc.) represent the barycenters of related two-body systems. Blue (orange) line represents gravitation that controls

these asteroids. Large black arrow represents the mean motion of asteroid belt, while short blue (orange) arrow represents mean motion of each family.

The formation of asteroid belt is numerically determined. However, before the beginning of this work, we must know that at the moment when the collision of the two bodies of binary planetary (satellite) system occurs, all fragments must instantaneously hold one inertial motion, while the collision subsequently gives each fragment another motion. This means that, the final motion of each fragment is a consequence of the interaction of inertial motion and gravitation. This may be approximated that each fragment is being dragged to run a parabolic trajectory around a gravitation origin (Fig.3). But because the gravitation origin is always in motion, the parabolic trajectory is dragged to distort in space.

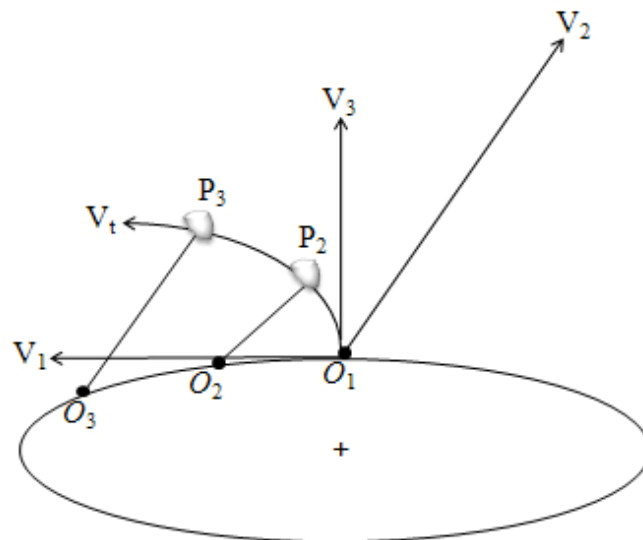


Figure 3: Fragment's motion under the interaction of inertial motion and gravitation. A fragment is ejected from a gravitation origin O_1 , at the moment the fragment's inertial motion is V_1 that is tangential to the position of O_1 , the motion obtained from the collisional ejection is V_2 , the composite motion between the two is V_3 , but because of the effect of gravitation that is from the origin O_1 and the origin is in motion along a path O_1 - O_2 - O_3 , the fragment is therefore dragged to run a parabolic trajectory of O_1 - P_2 - P_3 .

And then, we assumed that some nearby fragments are being confined to fall on a circular belt around the center body (Fig. 4(A)). To specify this confinement, we define a

three-dimensional Cartesian coordinate system, in which the barycenter (point O) is the origin, xoy plane is parallel to the orbital plane of the barycenter, and zoy plane is perpendicular to the orbital plane. We assumed that two branches of fragments are flatly distributed at xoy plane that is parallel to the ecliptic, while another two branches of fragments are flatly distributed at zoy plane that is vertical to the ecliptic (Fig. 4(B)). It has also been proposed that the gravitation between objects is promulgated through the barycenters of a series of two-body systems (Yang 2011). This means that the Sun and planets are indirectly attracting these fragments through the barycenters of related two-body systems. But because the Sun relative to planet has a very massive mass, the gravitational effect of all planets on fragment may be neglected, the Sun may be treated as the only gravitation origin.

According to (Fig. 4(B)), the motion of each fragment (barycenter) may be written as

$$V_t = \sqrt{V_0^2 + (at)^2 - 2 \times V_0 \times at \times \cos\alpha} \quad (1)$$

$$S_t = \frac{1}{2} \times a \times t^2 \quad (2)$$

$$X(Z)_t = S_t \times \cos\beta \quad (3)$$

Where a represents acceleration encountered by a fragment (barycenter), V_0 the initial velocity of the fragment (barycenter) at the moment when the collision occurs (which is virtually a consequence of the interaction of inertial motion and ejection motion), V_t the orbital velocity of the fragment (barycenter) after a time of t , S_t the displacement of the fragment (barycenter) that is from the influence of gravitation, $X(Z)_t$ the displacement of the fragment (barycenter) in the direction of x (z) axis, α the angle between the initial velocity and gravitation, β the angle between x axis and gravitation.

For example, at any moment fragment M_9 encounters a gravitation that is from other fragments and the Sun, the Sun's gravitation runs a path of Sun- O - a - d - e - f - M_9 , therefore the gravitational distance between the Sun and M_9 is $L_{\text{Sun-M}_9} = L_{\text{Sun-O}} + L_{O-a} + L_{a-d} + L_{d-e} + L_{e-f} + L_{f-M_9}$, while fragment M_{18} 's gravitation runs a path of M_{18} - 7 - 5 - 4 - 1 - O - a - d - e - f - M_9 , which corresponds to a gravitational distance of $L_{M_{18-M_9}} = L_{M_{18-7}} + L_{7-5} + L_{5-4} + L_{4-1} + L_{1-O} + L_{O-a} + L_{a-d} + L_{d-e} + L_{e-f} + L_{f-M_9}$. The fragment's initial velocity is V_0 , the gravitation is in the direction of line M_9 - f , the interaction of initial motion and gravitation thus makes M_9 move momentarily in the direction of line M_9 - D , even if the gravitation can contribute some work to make M_9 move towards y axis. This situation

is the same for all other fragments.

The acceleration is here determined by an experienced method, because if we simply treat $g = a$ (where g is gravitational acceleration), the Sun will swallow the Earth quickly, this is obviously not the fact. But we can strongly make sense, the acceleration is essentially derived from a cause of gravitation, therefore there must be a relation between them. In another work (unpublished), I employ a geological record of coral fossil to estimate the orbital decreasing rate of planet and satellite, which reflects the relation of acceleration and gravitation. The orbital decreasing rate for the Earth is $\Delta R_{\text{earth}} = 12.15 \times 10^{-5} \times t + \frac{1}{2} \times 8.3681 \times 10^{-16} \times t^2$ km (where the unit of t is in days). Assumed that the orbital decreasing rate is exponentially relative to gravitational distance and mass if they are from the same gravitation origin, the orbital decreasing rate for the barycenter (point O) in this paper may be written as $\Delta R_O = \left(\frac{R_{\text{earth}}}{R_O}\right)^2 \times \Delta R_{\text{earth}}$ (where R_{Earth} is the orbital radius of the Earth-Moon system around the Sun that is equal to 1 AU, R_O the orbital radius of asteroid belt that is assumed to be 2.67 AU, this value will be discussed in the last chapter). As the collision of the binary planetary system occurred 3.9 billion years ago, this means that, at the moment the orbital radius of the binary planetary system around the Sun is $R_O = 2.67$ (present) + $0.14 \times \Delta R_{\text{earth}}$ (past) = 4.13 AU, which is equal to $L_{\text{Sun-O}}$. We further define $\Delta R_O = \bar{a}t$ to obtain an average acceleration for the barycenter (point O). As the fragments (barycenters) are constrained by the same gravitation origin-the Sun, the acceleration for each fragment (barycenter) may be further written as $a = \bar{a} \times \left(\frac{L_{\text{Sun-O}}}{L_{\text{Sun-fragment}}}\right)^2$. The initial positions of fragments (barycenters) and their mass are assigned in Table 1, the unit of the coordinate axis is AU and 1AU = 149 598 000 km, and given the gravitation between any two fragments is slight if their distance is large enough, the Sun's gravitation is the only one that attracts each fragment. The displacement of fragment that is from the influence of gravitation is thus determined (Fig.5).

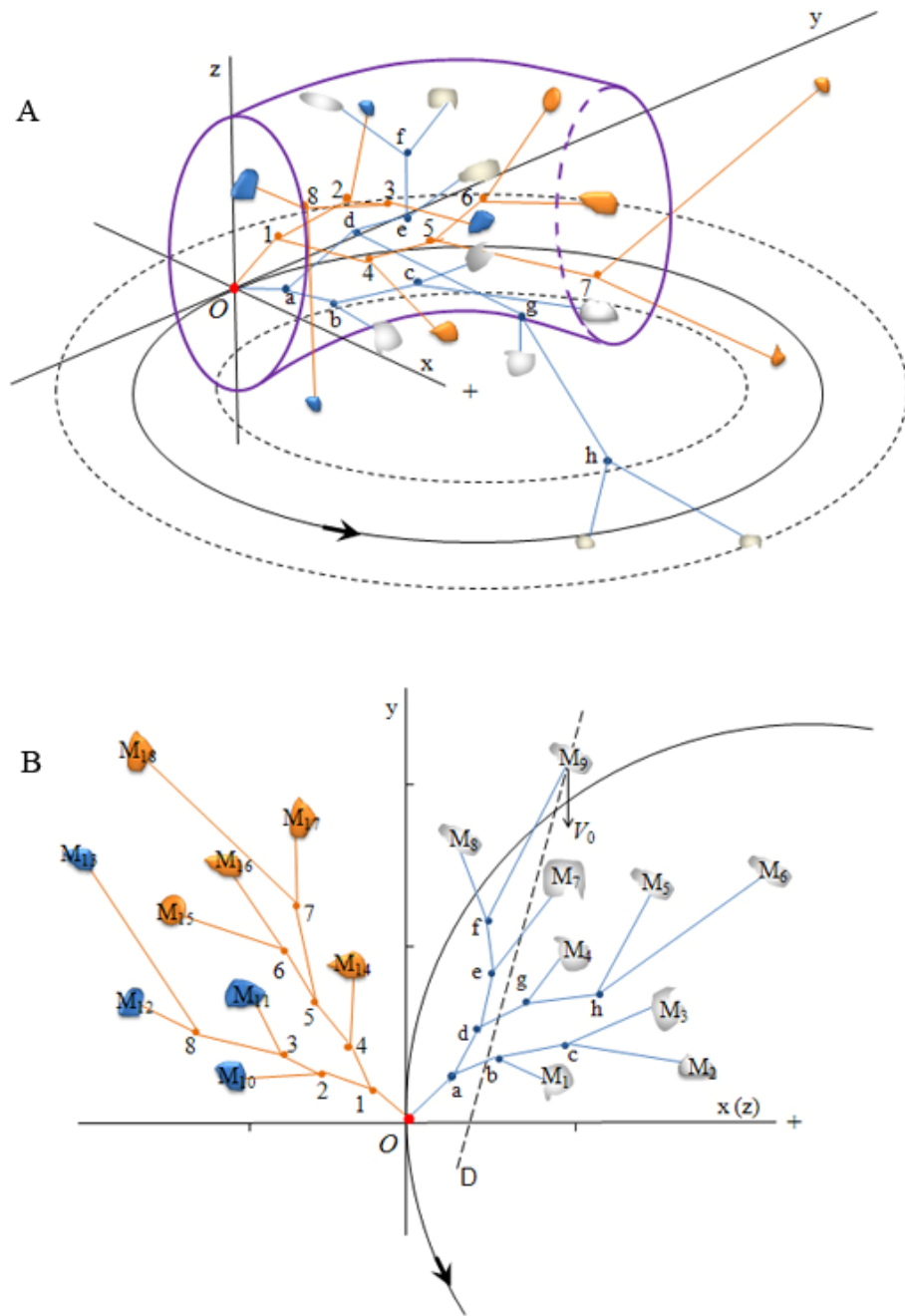


Figure 4: Fragment's modeling arrangement A: fragments are being organized into a series of hierarchical two-body systems to orbit. Point O is the barycenter that is survived in the collision. xoy plane is approximately parallel to the ecliptic, while zoy plane is vertical to the ecliptic. Curved cylinder represents a spatial distribution of fragments; B: four branches of fragments are ideally assigned at xoy , $-xoy$, zoy , and $-zoy$ plane, respectively. Note each branch here represents two. y axis is always tangential to the orbit of the barycenter (point O).

The result shows the fragments under the constraint of a series of hierarchical two-body gravitation run a very lengthy falling. In the direction of z axis, after a time of 3.9 billion years 83% the sample fragments fall into a distance of less than 0.15 AU from the ecliptic. With the passage of time, the spatial region of these fragments in the vertical direction becomes thinner and thinner. Contrary to this, in the direction of x axis, during a time of 2.3 billion years these sample fragments are always approaching the orbit of the barycenter (point O), by which the spatial region of these fragments is radially depressed (the least width of the region is around 0.56 AU), but when the right branch of fragments $M_1\sim M_9$ ride over the orbit of the barycenter (point O), the radially differential motion between these fragments and barycenters can lead them to spread out, by which the region becomes wider and wider, even if these fragments are always approaching the orbit of the barycenter (point O). The longitudinal differential motion between these fragments can also lead them to spread out, by which the region is stretched into a full circle around the Sun. The time of forming such a circle may be expressed as

$$t = \frac{2\pi}{\left(\frac{\sqrt{V_1^2 + (a_1 t)^2 - 2 \times V_1 \times a_1 t \times \cos \alpha_1}}{R_1} - \frac{\sqrt{V_2^2 + (a_2 t)^2 - 2 \times V_2 \times a_2 t \times \cos \alpha_2}}{R_2} \right)} \quad (\text{where } V_1 \text{ and } V_2 \text{ are}$$

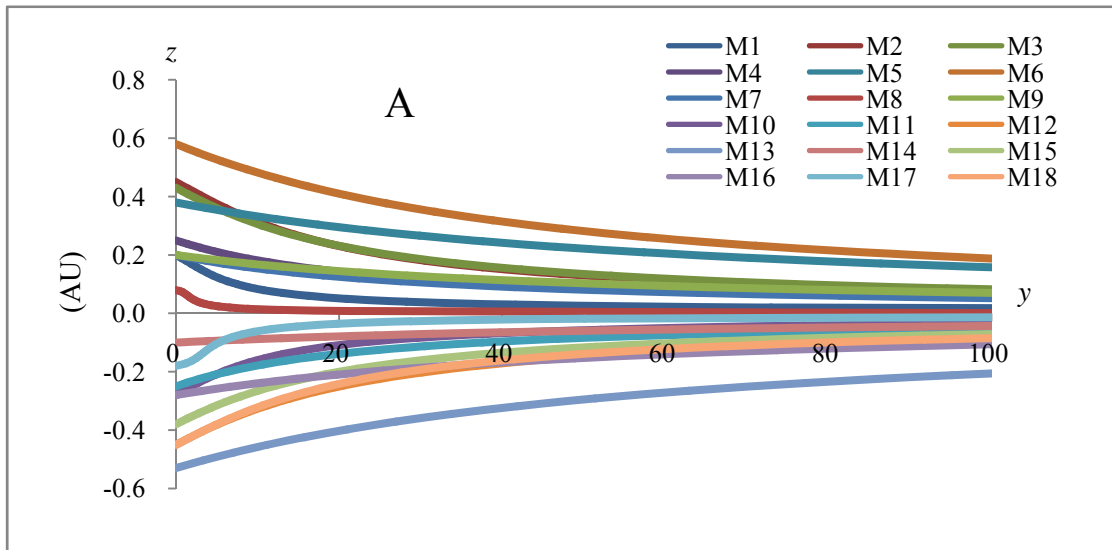
respectively the initial velocity of two fragments, a_1 and a_2 respectively acceleration, α_1 and α_2 respectively the angle between the tangential velocity and gravitation, R_1 and R_2 the orbital radius, each fragment is assumed to approximately take a velocity of V to run a circle of radius R around the Sun). According to Figure 4 and Table 1, in the left branch of fragments $L_{O-M14} = 0.263$ AU, $R_{O-M14} = 0.1$ AU, $L_{O-M18} = 0.738$ AU, $R_{O-M18} = 0.45$ AU, where R_{O-M14} and R_{O-M18} are the radial distance between the fragment and the barycenter (point O), respectively, the two are the nearest and most distant, respectively, fragment M_{14} therefore is the fastest to longitudinally catch up with fragment M_{18} than other fragments. The time for the circle's formation is worked out to be

91.51 years on the assumptions that $a_1 = \bar{a} \times \left(\frac{R_o}{L_{\text{Sun}-M14}}\right)^2$, $a_2 = \bar{a} \times \left(\frac{R_o}{L_{\text{Sun}-M18}}\right)^2$, $\alpha_1 = \alpha_2 = 20^\circ$,

$$V_1 = \sqrt{\frac{GM_{\text{Sun}}}{L_{\text{Sun}-o} + R_{O-M14}}}, \quad V_2 = \sqrt{\frac{GM_{\text{Sun}}}{L_{\text{Sun}-o} + R_{O-M18}}}, \quad G = 6.67 \times 10^{-11} \text{ m}^3 \text{ kg}^{-1} \text{ s}^{-2}, \quad M_{\text{Sun}} = 1.99 \times 10^{30} \text{ kg}.$$

Observation shows that the major part of asteroid belt is currently from 2.15 to 3.3 AU. In this simulation the 18 sample fragments selected are initially assigned at a range of less than 0.8 AU from the collisional origin, they at present evolve into a belt of approximately 2.77 AU \sim 3.45 AU from the Sun. This suggests that the radial distribution of sample fragments in the model

might be too narrow, especially for the right branch of fragments. We should not forget that in the simulation the present distance of the barycenter of initial binary planetary system from the Sun is defined as $R_0 = 2.67$ AU, this value is from an average of the semi-axis of main belt asteroids. The radial immigration suggests that the actual position of the barycenter of initial binary planetary system at present should be either at the inner edge of main belt or below it. If so, we may match the belt width between simulation and observation by means of reducing the amplitude of R_0 . Moreover, fragments are randomly ejected from the collisional origin and then are spherically distributed, the fragments in Figure 4(B) are only a few representatives of countless fragments. In practice, the majority of the fragments are distributed neither in the xoy plane nor in the zoy plane, instead, they are distributed freely between the four branches of fragments. But anyway, a hierarchical two-body confinement mechanism may make fragments form asteroid belt. It is necessary to note that we consider only the confinement that is derived from the effect of gravitation, the influence of inertial motion is not included.



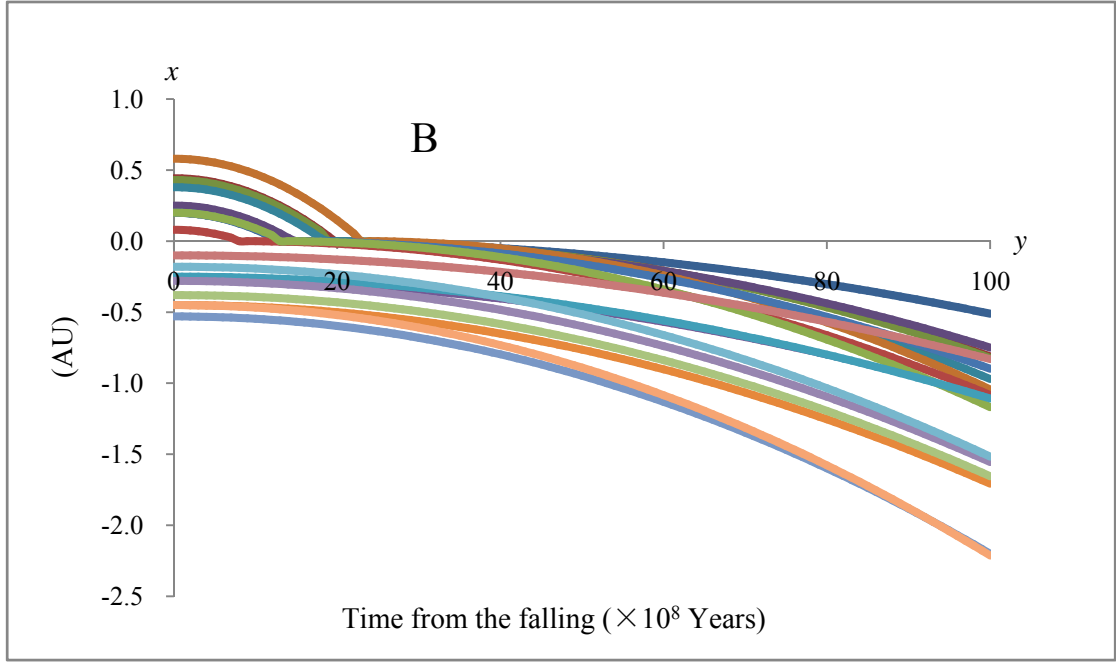


Figure 5: Fragment's confining motion. A: fragments are vertically falling on xoy plane that is parallel to the ecliptic; B: fragments are radially approaching the orbit of the barycenter (point O) that is always tangential to y axis. The present is at the time of 3.9 billion years.

Barycenter and fragment	Coordinate		Mass (m)
	$x(z)$	y	
O	0.00	0.00	1.00
a	0.08	0.08	0.30
b	0.15	0.10	0.15
c	0.25	0.11	0.05
d	0.10	0.13	0.15
e	0.13	0.20	0.07
f	0.13	0.28	0.03
g	0.18	0.15	0.08
h	0.30	0.16	0.04
1	0.05	0.05	0.70
2	0.13	0.08	0.57
3	0.20	0.11	0.27
4	0.10	0.11	0.13
5	0.15	0.18	0.11
6	0.23	0.25	0.04
7	0.21	0.33	0.07
8	0.35	0.13	0.07
M_1	0.20	0.08	0.10
M_2	0.45	0.10	0.03
M_3	0.43	0.15	0.02

M ₄	0.25	0.25	0.04
M ₅	0.38	0.35	0.03
M ₆	0.58	0.38	0.01
M ₇	0.20	0.38	0.02
M ₈	0.08	0.43	0.01
M ₉	0.20	0.55	0.04
M ₁₀	-0.28	0.08	0.30
M ₁₁	-0.25	0.18	0.20
M ₁₂	-0.45	0.15	0.03
M ₁₃	-0.53	0.38	0.04
M ₁₄	-0.10	0.23	0.02
M ₁₅	-0.38	0.30	0.03
M ₁₆	-0.28	0.40	0.01
M ₁₇	-0.18	0.45	0.06
M ₁₈	-0.45	0.58	0.01

Table 1: Parameter assignment for fragments (barycenters) in the model. $1m = 70\%$ the mass of the binary planetary (satellite) system. Note that the majority of the mass of the two bodies after their disruption is considered to be distributed at a small spatial region.

Estimate of shattering energy for the binary planetary system follows this process. Due to $M_{\text{Earth}} = 5.97 \times 10^{24}$ kg, $M_{\text{Moon}} = 7.35 \times 10^{22}$ kg, $L_{\text{Earth-Moon}} = 384\,000$ km, $P_{\text{Moon}} = 27.32$ days, $R_{\text{Earth}} = 6\,370$ km, $R_{\text{Moon}} = 1\,738$ km (where M_{Earth} and M_{Moon} are respectively the mass of the Earth and Moon, $L_{\text{Earth-Moon}}$ is the distance between the Earth and Moon, P_{Moon} is the orbital period of the Moon, R_{Earth} and R_{Moon} are respectively the radius of the Earth and Moon), thus the orbital radius of the Moon in the Earth-Moon system is $L_{\text{Moon}} = (M_{\text{Earth}} \times L_{\text{Earth-Moon}}) / (M_{\text{Earth}} + M_{\text{Moon}}) = 379\,330$ km, the orbital velocity is $V_{\text{Moon}} = 2\pi L_{\text{Moon}} / P_{\text{Moon}} = 1.0$ km s⁻¹, the orbital radius of the Earth in the Earth-Moon system will be $L_{\text{Earth}} = L_{\text{Earth-Moon}} - L_{\text{Moon}} = 4\,670$ km, the orbital velocity is $V_{\text{Earth}} = L_{\text{Earth}} \times V_{\text{Moon}} / L_{\text{Moon}} = 0.012$ km s⁻¹. The kinetic energy for the Earth-Moon system will be $E_k = (M_{\text{Earth}} \times V_{\text{Earth}}^2 + M_{\text{Moon}} \times V_{\text{Moon}}^2) / 2 = 3.72 \times 10^{28}$ J. When the Moon collides with the Earth, their gravitational potential is converted to kinetic energy, thus $E_p = GM_{\text{Earth}} M_{\text{Moon}} [(1/L_{\text{Moon}1} - 1/L_{\text{Moon}2}) + (1/L_{\text{Earth}1} - 1/L_{\text{Earth}2})]$ (where $L_{\text{Moon}1}$ is the gravitational distance of the Moon to the barycenter of Earth-Moon system when the collision occurs, $L_{\text{Moon}2}$ the initial gravitational distance, $L_{\text{Earth}1}$ the gravitational distance of the Earth to the barycenter of Earth-Moon system when the collision occurs, $L_{\text{Earth}2}$ the initial gravitational distance. After a deduction, $L_{\text{Moon}1} = 8\,009$ km, $L_{\text{Moon}2} = 379\,330$ km, $L_{\text{Earth}1} = 98$ km, $L_{\text{Earth}2} = 4\,670$ km), thus the gravitational potential work is worked out to

be $E_p = 2.93 \times 10^{32}$ J. Also note that in the frame of hierarchical two-body system the Sun and other planets are exerting gravitation to the Earth and Moon by means of the barycenters of a series of hierarchical two-body systems, but at a large distance other planet's effect on the Earth and Moon may be overlooked. As a result, the Sun's gravitational work to the Earth and Moon is $E_{\text{Sun}} = GM_{\text{Sun}} \times [M_{\text{Moon}}(1/L_{\text{Moon-Sun1}} - 1/L_{\text{Moon-Sun2}}) + M_{\text{Earth}}(1/L_{\text{Earth-Sun1}} - 1/L_{\text{Earth-Sun2}})] = 3.23 \times 10^{29}$ J, where $G = 6.67 \times 10^{-11} \text{ m}^3 \text{ kg}^{-1} \text{ s}^{-2}$, $M_{\text{Sun}} = 1.9891 \times 10^{30}$ kg, $L_{\text{Moon-Sun1}}$ is the gravitational distance of the Moon to the Sun (that is equal to $L_{\text{Moon1}} + L_{\text{bary-Sun}} \approx 8\,009 + 149\,598\,000 = 149\,606\,009$ km) when the collision occurs, $L_{\text{Moon-Sun2}}$ the initial gravitational distance (that is equal to $L_{\text{Moon2}} + L_{\text{bary-Sun}} \approx 379\,330 + 149\,598\,000 = 149\,977\,330$ km), $L_{\text{Earth-Sun1}}$ the gravitational distance of the Earth to the Sun (that is equal to $L_{\text{Earth1}} + L_{\text{bary-Sun}} \approx 98 + 149\,598\,000 = 149\,598\,098$ km) when the collision occurs, $L_{\text{Earth-Sun2}}$ the initial gravitational distance (that is equal to $L_{\text{Earth2}} + L_{\text{bary-Sun}} \approx 4\,670 + 149\,598\,000 = 149\,602\,670$ km). The total energy for the Earth-Moon system at the moment when the collision occurs will be $E = E_k + E_p + E_{\text{Sun}} \approx 2.93 \times 10^{32}$ J (we assumed that the collision occurs at the moment when $L_{\text{earth-moon}} = R_{\text{earth}} + R_{\text{moon}} = 8\,108$ km). Such a quantity of energy is powerful enough to shatter the two bodies of the binary planetary system into small fragments.

It can be inferred that under the frame of hierarchical two-body association, every fragment will hold a companion that is either a fragment or an association of a series of hierarchical two-body systems of small fragments. This point has been partially proved by observation. Nearly all of the solar system's small-body reservoirs have been found to hold binaries (Funato et al. 2004; Durda et al. 2006; Weidenschilling, 2002; Goldreich et al. 2002; Astakhov et al. 2005; Canup 2005). Recent surveys discovered that ~16% of near-Earth asteroids, ~2% of large main-belt asteroids, and ~11% of Kuiper-belt objects are being orbited by satellites (Margot et al. 2002; Merline et al. 2002; Stephens and Noll 2006). Given the observational limitation in time and instrument, we still have chance to find more binaries in the future.

3.2 Planetary ring

Observation shows that the rings of each giant planet are mutually parallel and there are many divisions within them. For example, Cassini division, Roche division, and so on are in the Saturn's rings. The voids between the rings of Uranus and Neptune may be treated as divisions. These divisions look like natural boundaries, and the particles in each ring appear to be never ride

over them. A broad, flat profile is common, for example, the Jupiter's rings, the Saturn's rings, Uranus's 1986U2R/ ζ , ν and μ rings, and the Neptune's Galle, and Lassell rings. Many irregularly shaped satellites have been found within (or in) the planetary rings. For example, Adrastea and Metis are embedded in the Jupiter's main ring, while Amalthea is embedded in the Gossamer ring. Mimas, Enceladus, and Tethys are embedded in the Saturn's E ring. Cordelia, Ophelia, Bianca, Cressida, Desdemona, Portia, Rosalind, Cupid, Belinda, Perdita, and Puck are embedded within (or in) the Uranus's rings. Naiad, Thalassa, Despina, Galatea, and Larissa are within the Neptune's rings. The structure of moonlet and clump has also been detected in the rings (Esposito et al. 2008). It has been already observed that the Saturn's rings have different spectral characteristics that are parallel to one another. Figure 6 shows the appearances of three giant planets' ring systems.

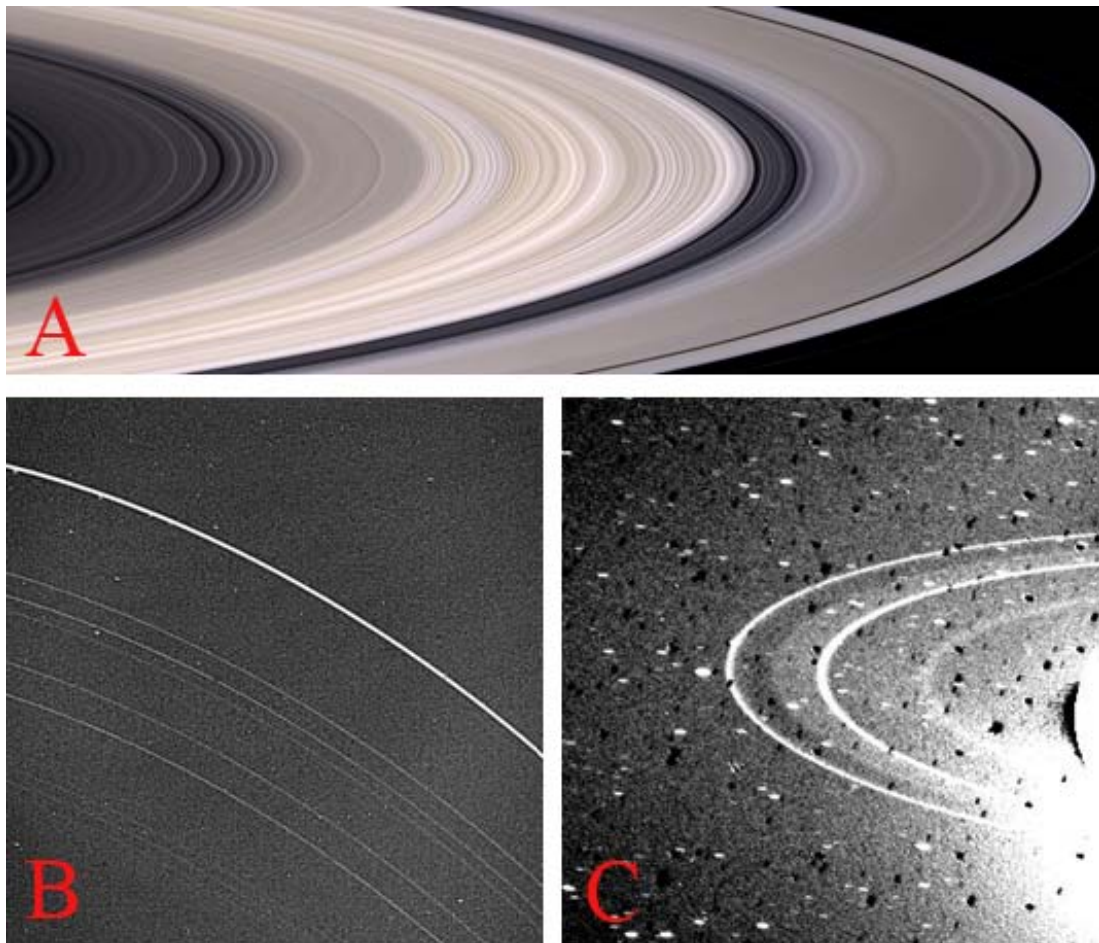


Figure 6: General view of several giant planets' ring systems. A: Saturn Rings taken 12 December 2004; B: Voyager 2's picture of Uranus' rings taken on 22 January 1986; C: Voyager 2 picture of Neptune's rings taken on 26 August 1989. Credit: NASA/JPL/Space Science Institute.

Reference to Figure 1, we replace the two-body system with a binary satellite system and the center body with a giant planet. It can be inferred that, after the disruptive collision of the two bodies, some of the falling fragments may be further shattered into very small fragments (particles with a size of meter or micron, for instance) that are still organized in a series of hierarchical two-body systems. Similar to the situation of asteroid family (or group), the small fragments that are from the disruption of a parent body may form a physical association, with the passage of time, the longitudinally differential motion between these small fragments will lead them to stretch and eventually form a full ring around the planet. The disruptions of many fragments at the same time may form many full rings around the planet. The non-disrupted fragments are left to be embedded in (within) the rings to orbit together, by which they are called shepherds. Given the orbital decrease as proposed (Yang 2011), the survived barycenter will continue to orbit and drag these rings of small fragments to radially immigrate towards the planet, the radially differential motion will make the rings slowly become flat. As the fragments are spatially separated, there must form a division between any adjacent two rings. Also because the small fragments of each ring are dragged by a leading barycenter and the barycenters of a series of subordinate hierarchical two-body systems, the parallel, independent rings are determined. As the two bodies of binary satellite system are composed of different materials, different fragments ejected may thus hold different proportional materials, and then, if they are further shattered into very small fragments to form independent rings, different spectral characteristics are determined for the rings. Reference to Figure 4, the fragments distributed at the xoy plane can make only radial immigration, while the fragments distributed at the zoy plane can make not only radial immigration but also vertical falling, this means that the distribution of different material fragments may be randomly crossbedded together. However, if the disruption of a fragment is not in depth, the residual may be embedded in the ring to create the structure of moonlet and clump. Figure 7 demonstrates an artistic configuration of planetary ring system, in which all fragments are being organized in a series of hierarchical two-body systems to orbit. The planet's gravitation mainly controls the motions of these fragments by means of the barycenter of initial binary satellite system (point O) and the barycenters of a series of subordinate hierarchical two-body systems. Simply speaking, the motion of each particle in the ring is a consequence of the interaction of inertia and gravitation,

in which the inertia keeps the particle to move in a straight line, but the gravitation forever drags it to deviate from the straight line, a curving motion for the particle is therefore maintained.

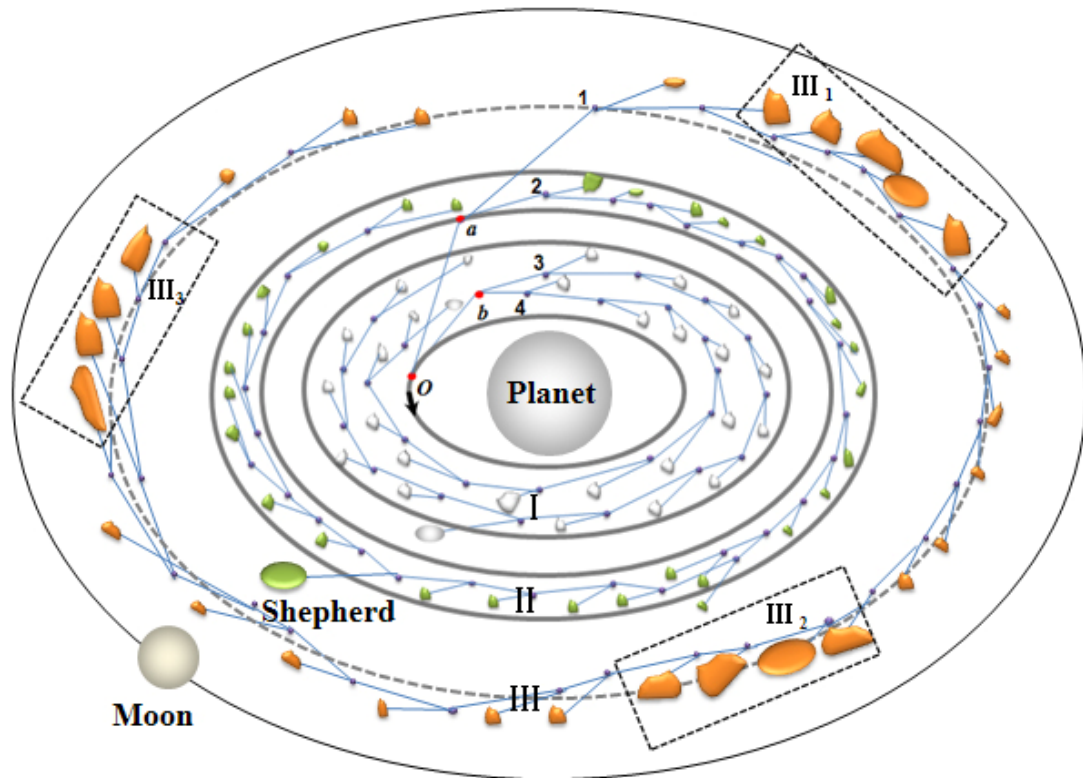


Figure 7: A hierarchical two-body association of fragments for planetary ring system. Planet is equivalent to Jupiter, Saturn, Uranus, and Neptune, respectively; I is equivalent to planet's broad rings like Gossamer rings of Jupiter, A, B, C, D, and E rings of Saturn; II is equivalent to planet's general rings like Janus/Epimetheus, G, and Pallene rings of Saturn, 1986U2R/ ζ and μ rings of Uranus, Lassell ring of Neptune; III is equivalent to planet's narrow rings like F ring of Saturn, 6, 5, 4, α , β , η , γ , δ , λ , ϵ , ν rings of Uranus, Galle, Le Verrier, and Adams rings of Neptune; I₁, II₂, and III₃ is equivalent to ring arcs (clumps) like Methone and Anthe arcs of Saturn, Fraternité, Égalité 1, Égalité 2, Liberté, and Courage arcs of Neptune. Any two adjacent rings are naturally divided by division. Point O is the barycenter of integral ring system that drags point a and b to orbit, at the same time point a drags point 1 and 2 to orbit, point b drags point 3 and 4 to orbit, while point 1, 2, 3, and 4 respectively drags a series of subordinate hierarchical two-body systems of small fragments to orbit, by which a ring system is formed around the planet. Red (brown) dot denotes the barycenter of related two-body system, blue line denotes gravitation. Large black arrow denotes the mean motion of integral ring system. Different color in the ring system denotes different chemical composition.

We use the parameters of Figure 4 and Table 1 and equations (1)(2)(3) to quantify the formation of the Saturn's ring system. The center body is replaced with the Saturn. The coordinate unit is million kilometers. As the Sun's gravitation to planet is different from planet's gravitation to satellite, the relation of acceleration and gravitation for satellite needs to be recalculated. Similarly, the orbital decreasing rate of the Moon from another work was $\Delta R_{\text{Moon}} = 4.4583 \times 10^{-7} \times t + \frac{1}{2} \times 3.071 \times 10^{-18} \times t^2$ km (where the unit of t is in days). Given the relation of acceleration and gravitation for the Moon may be expressed as $\Delta R_{\text{Moon}} \sim \frac{GM_{\text{Earth}}}{L_{\text{Earth-Moon}}^2}$, which is applicable for any planet and its satellite, the orbital decreasing rate for the binary satellite system may thus be written as

$$\Delta R_{\text{O}} = \frac{M_{\text{Saturn}}}{M_{\text{Earth}}} \times \left(\frac{L_{\text{Earth-Moon}}}{L_{\text{Saturn-O}}}\right)^2 \times \Delta R_{\text{Moon}} = 13.74 \times (4.4583 \times 10^{-7} \times t + \frac{1}{2} \times 3.071 \times 10^{-18} \times t^2)$$

if $L_{\text{Saturn-O}} = 1\,000\,000$ km (where $M_{\text{Earth}} = 5.97 \times 10^{24}$ kg, $M_{\text{Saturn}} = 5.68 \times 10^{26}$ kg, $L_{\text{Earth-Moon}} = 380\,000$ km). We further define $\Delta R_{\text{O}} = \bar{a}t$ to obtain an average acceleration for the binary satellite system. Given all fragments are constrained by the same gravitation origin-the Saturn, the acceleration for each fragment may be further expressed as $a = \bar{a} \times \left(\frac{L_{\text{Saturn-O}}}{L_{\text{Saturn-fragment}}}\right)^2$.

Initial velocity of a fragment is assumed to be $V_0 = \sqrt{\frac{GM_{\text{Saturn}}}{L_{\text{Saturn-fragment}}}}$ (where the Saturn's mass $M_{\text{Saturn}} = 5.68 \times 10^{26}$ kg, $L_{\text{Saturn-fragment}}$ is the distance of a fragment and the Saturn). The Saturn's gravitation to the binary satellite system here is thought to be primary because the Sun is too distant. We further assumed that the majority of the fragments in motion are disrupted into very small fragments (the size of water particles, for example) that are still organized in a series of hierarchical two-body systems to form independent rings. As shown in Figure 8 and 9, the fragments in the direction of z axis run a very lengthy falling, during a period of 2 billion years, they fall into a distance of less than 10 000 km from xoy plane (that is approximately parallel to the Saturn's equatorial plane), some of them may even reach a distance of less than several kilometers. In the direction of x axis (that is directed towards the Saturn) the right branch of fragments ($M_1 \sim M_9$, for example) take a time of approximately 180 million years to reach the orbit of the barycenter (point O), during this period the left branch of fragments ($M_{10} \sim M_{18}$, for example) due to radially differential motion are radially spread out, even though they are approaching the planet forever. Around 300 million years later, the orbit of the barycenter (point O) immigrates to

a distance of 137 000 km from the planet, the width of all fragments varies from 1 110 000 to 1 040 000 million kilometers. Among of them, the nearest fragment (M_2) is at a distance of 137 000 km from the planet, while the furthestmost fragment (M_{13}) is at a distance of 1 230 000 km from the planet. The vertical falling and radial immigration together make the spatial region of these fragments flat. As the binary satellite system is initially composed of mainly ice + silicate + oxygen, icy rings may thus be determined. Unlike the fragments of binary planetary system that are responsible for the formation of asteroid belt, every fragment here may form an independent ring when disrupted. Unfortunately, the time for disrupting a fragment is unknown, the timescale of forming a full ring is therefore hard to quantify. The mass and disruptive severity of a fragment controls the width of a ring that forms from it, but it cannot be quantified here, too. The creation of a ring may be roughly expressed by Figure 4 (B) that a moving fragment due to disruption forms a configuration of the left branch of fragments (M_{10} - M_{18} , for instance) that are still organized in a series of hierarchical two-body systems, the longitudinally differential motion between these fragments leads them to stretch and forms a full ring around the center body, while the radially differential motion leads them to spread out and makes the ring flat. The simulation also reflects a fact that the vertical falling relative to radial immigration is too slow. This suggests that the binary satellite system be at a distance of far larger than 1 000 000 km from the Saturn when the collision of its two bodies occurred. The distance must be large enough for the barycenter of initial binary satellite system to radially immigrate during a time of billions of years. Similarly, in the simulation we consider only the confining motion that is derived from gravitation, the influence of inertial motion is not included. Table 2 shows a radial timescale for the formation of the Saturn's rings.

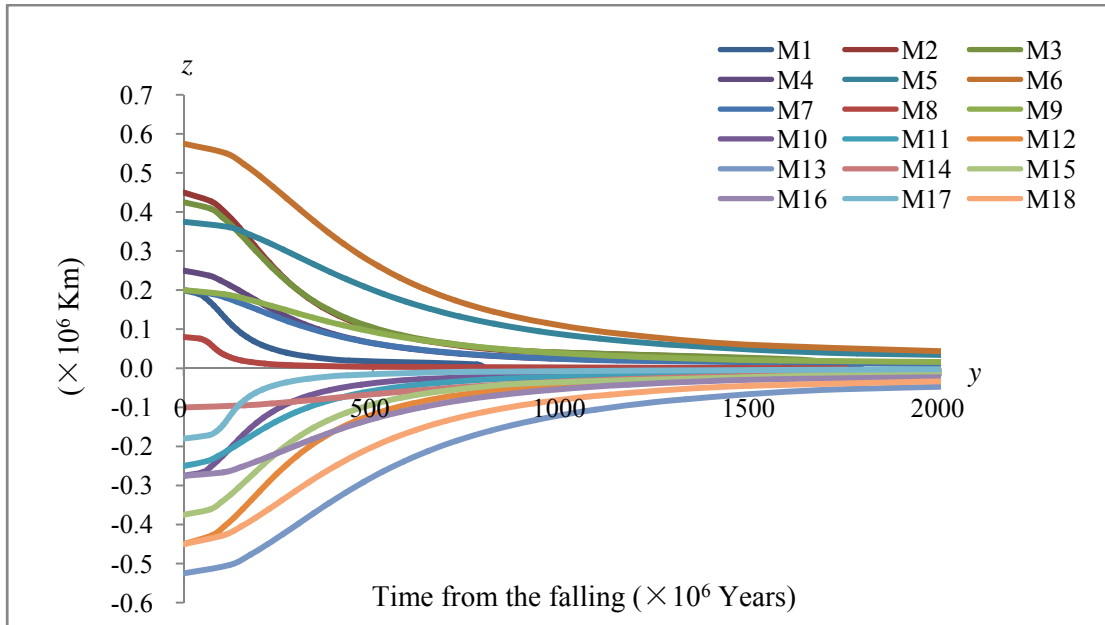


Figure 8: Fragment's vertical confinement. All fragments distributed in the direction of z axis are slowly falling on xoy plane that is parallel to the Saturn's equatorial plane, by which the rings become thinner and thinner.

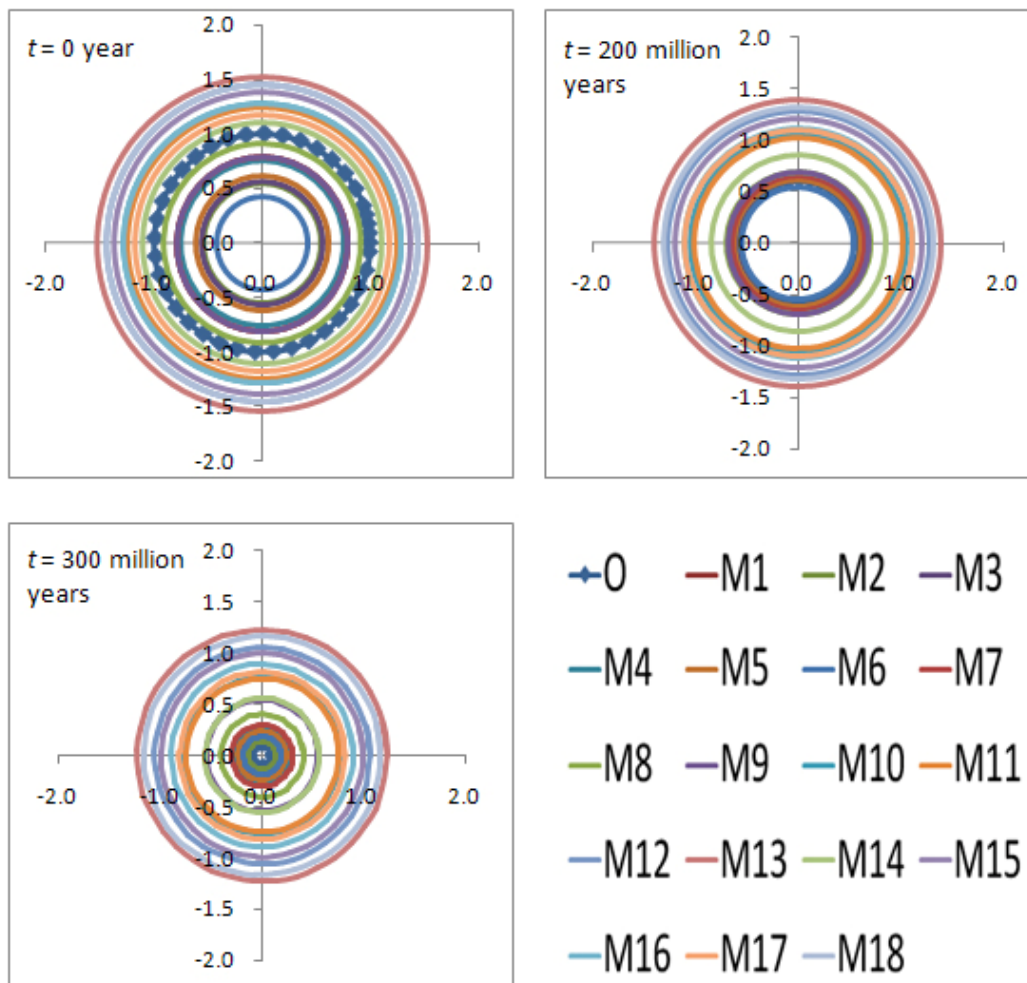


Figure 9: Orbital radial immigration of fragments (rings). The Saturn is at the center of the coordinate frame. The unit is million kilometers. Note that, because some of the fragments can be further shattered into smaller fragments to form independent rings, the orbit of each fragment may represent the orbit of a ring.

Ring name	Distance from Saturn's center (km)	Width (km)	Ro (km)	$L_{M14-M18}$	Time ($\times 10^6$ years)
D	66,900 – 74,510	7,500	66,900	350	704
C	74,658 – 92,000	17,500	74,658	350	1,327
B	92,000 – 117,580	25,500	92,000	350	1,889
A	122,170 – 136,775	14,600	122,170	350	1,592
G	166,000 – 175,000	9,000	166,000	350	1,414

Table 2: Radial formation timescale for the Saturn's rings. Assumed that the barycenter (point O) of the initial binary satellite system is now located at the inner edge of D ring, its distance from the Saturn is 66 900 km, which corresponds to an orbital decreasing rate of $\Delta Ro = 13.74 \times (4.4583 \times 10^{-7} \times t + 0.5 \times 3.071 \times 10^{-18} \times t^2)$, where the unit of t is in days. Every ring is derived from the disruption of a fragment and is closely controlled by a leading subordinate barycenter that is also located at the inner edge of the ring. The planet indirectly controls the particles of each ring through the barycenter (point O), the leading subordinate barycenter, and the barycenters of a series of interior hierarchical two-body systems. The particle assignment in the ring is similar to the configuration of the left branch of fragments in Figure 4(B). The coordinate unit in Table 1 is defined as 1000 km. M_{14} and M_{18} (relative to the planet) are considered to be respectively the nearest and furthestmost two particles in the ring. The orbital decreasing rate for each particle may be further expressed as $\Delta R_M = (L_{\text{Saturn-fragment}} / L_{\text{Saturn-o}})^2 \times \Delta Ro$ (where $L_{\text{Saturn-o}}$ represents the distance of the planet and the barycenter (point O), $L_{\text{Saturn-fragment}}$ the distance of the planet and the fragment, which is equal to the sum of the distance of leading subordinate barycenter to the planet and the distance of leading subordinate barycenter to the particle). The radial times for a ring's formation may thus be determined through a relation of $L_{\text{ring}} - L_{M14-M18} = (\Delta R_{M14} - \Delta R_{M18}) \times \sin \alpha$, where L_{ring} is the width of a ring, $L_{M14-M18}$ the initial radial distance between the two particles, α the angle between the tangential velocity and gravitation, which is assumed to be identical for the two particles and here is defined as 10° .

The simulation here suggests that the ring systems of Jupiter and Saturn are older than that of Uranus and Neptune, the faint, dusty Jupiter's ring system is likely to be older than the massive, spectacle Saturn's ring system, while the narrow Uranus's ring system should be younger than dark Neptune's ring system, and concludes that new rings are being created by the disruption of irregular satellites, narrow rings are being widening, and all rings due to orbital decrease will be eventually swallowed by the planets in the very distant future. Several expectations are provided to examine this model: 1) giant planet's rings are with various inclinations; and 2) the particles in a ring are as a body in motion, even if they are discontinuous in spatial distribution. To some extent, the whole planetary ring system and embedded satellites are as a body in motion.

The propeller-shaped and ringlet structures in the Saturn's ring and the twisted Fraternity arc in the Neptune's ring may be conceptually explained as follows (Fig.10): because the two bodies of a two-body system are derived from the disruptive collision of a parent body, after the disruption the two bodies will run parabolic trajectories around the common barycenter of their mass, but because this barycenter in the disruption is survived and continues to orbit, the parabolic trajectories can be dragged to distort, this makes them look like a two-armed propeller if they are embedded within (or in) the particles of the ring. If the two bodies are further shattered to form two associations of small particles, the two associations can also perform some kind of rotation, which makes them enlace with each other (like a twisted strand or rope). If only one body is shattered to form an association of small particles, the survived body will accompany the association to orbit together, which makes it look like a shepherd. Because of the rotation, each association of small particles itself looks like a long ringlet.

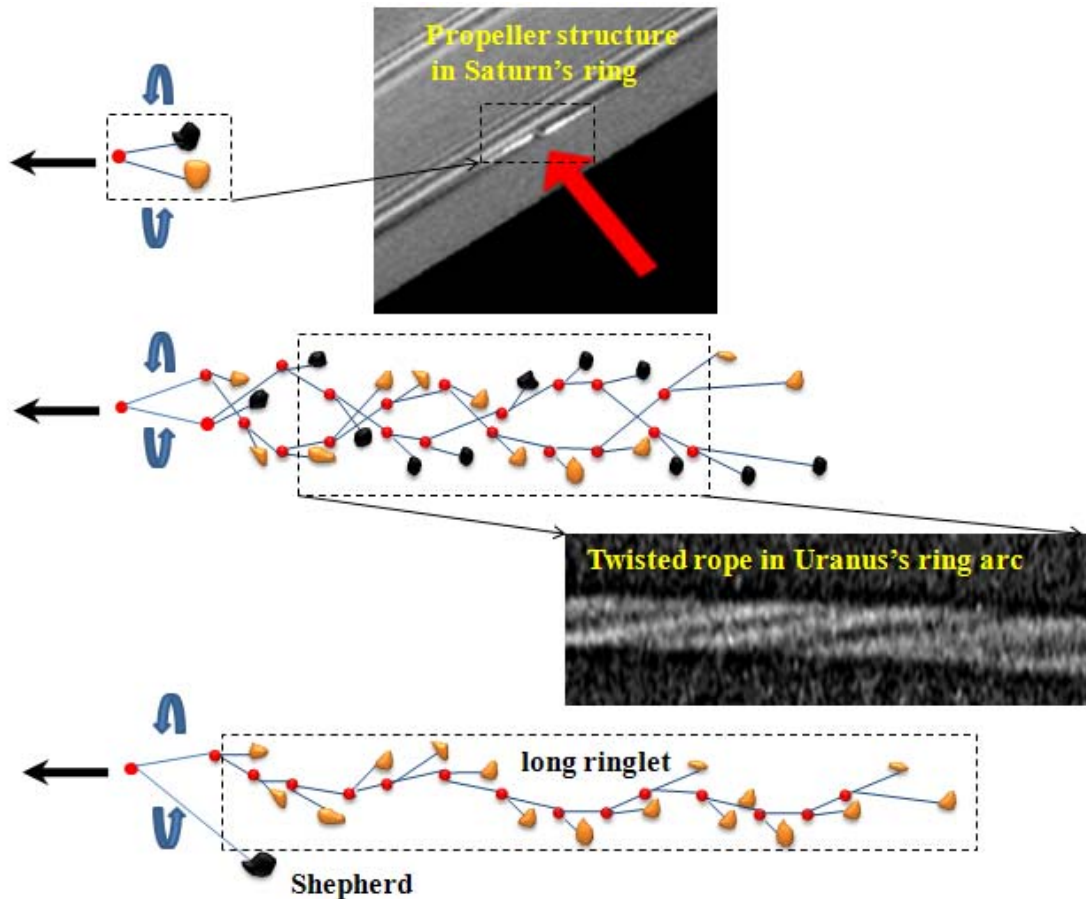


Figure 10: Modelling the formation of unusual structures. Top shows a moving rotational two-body system that fits to a propeller structure in Saturn's ring; Middle does a moving hierarchical two-body association of particles that fits to a twisted strand (rope) in Uranus's Fraternity arc. Also note that in the image there are at least three associations of particles to build up this twisted rope; Bottom does a moving two-body system that consists of a shepherd (satellite) and a long ringlet (a hierarchical two-body association of particles). Red dot denotes the barycenter of related two-body system. Large black arrow denotes the motion of an integral system (images by courtesy of NASA).

3.3 Comet

Observation shows that comets hold very eccentric movements that generally run cross the orbits of planets, and their orbital periods appear to be various, ranging from a few years to hundreds of thousands of years, and their bodies are volatile if close to the Sun enough. Galileo's experiment of projectile suggests that the fragments ejected from a collisional origin run some parabolic trajectories around the origin. We may infer that, if the projectile's speed is high enough, it may circle around the Earth, if the speed is very high, it will run a very big parabolic trajectory

to circle around the Earth, but anyway, the projectile due to the pull of the Earth's gravitation will eventually fall on the ground, even if it needs to take a long time to run many circles to finish this falling. This suggests that the fragments ejected from the collision of the two bodies of the binary planetary (satellite) systems will eventually fall back to the collisional origin. Reference to Figure 3, we know that every fragment is actually running a parabolic trajectory round a barycenter that is located in asteroid belt (or planetary ring), but because of the motion of the barycenter, the parabolic trajectory will be dragged to distort in space. Figure 11 shows such a fragment's orbit.

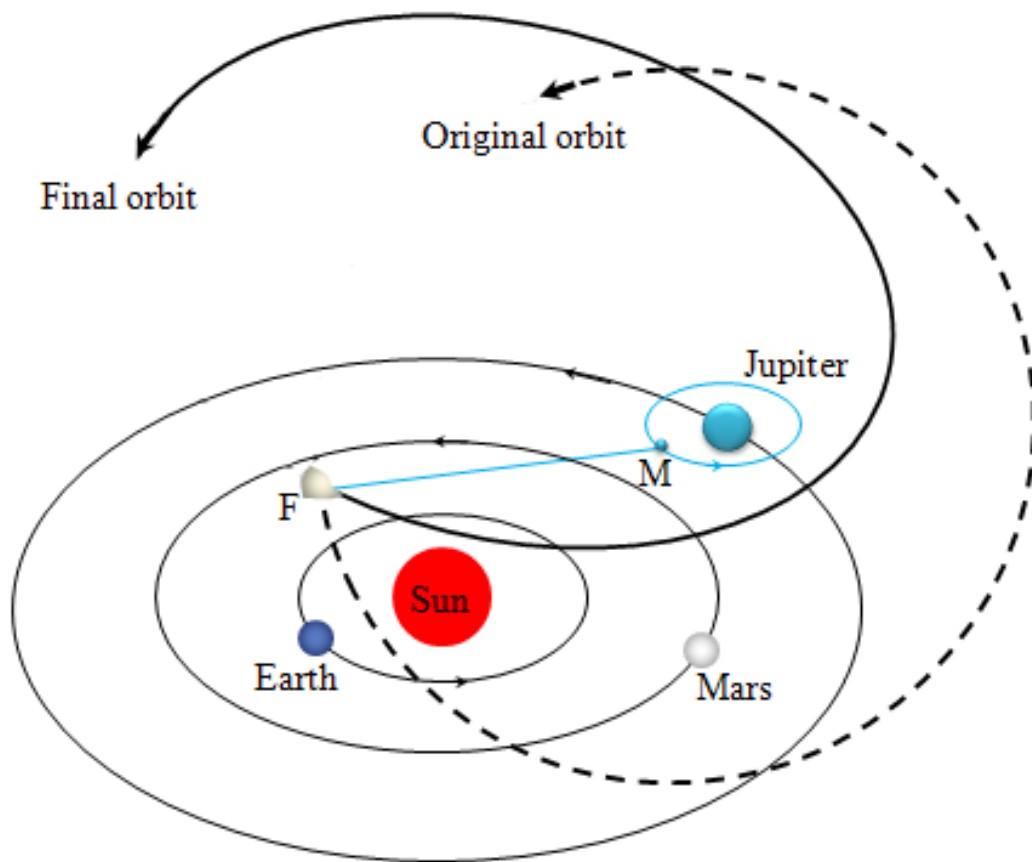


Figure 11: Trajectory of a fragment dominated by the Jupiter. The fragment (F) is falling on a barycenter (M) that is located in the Jupiter's ring system. Original orbit denotes the fragment is running a parabolic trajectory around the barycenter, while final orbit denotes the original orbit due to the motion of the Jupiter around the Sun is distorted.

Figure 12 shows that the fragments dominated by asteroid belt and four giant planetary ring systems cover the solar system extensively. In fact, if the orbital radius of a fragment is large enough, the falling towards the barycenter that is located in the ring may be treated as towards the

planet. Reference to Figure 11, when these fragments run some parabolic trajectories around the barycenters that are located in asteroid belt and giant planetary ring systems, they are at the same time being brought to move because of the motions of asteroid belt around the Sun and giant planets around the Sun. This makes their trajectories distorted. Once some of these fragments approach the Sun close enough, the Sun's radiation can warm them to become comets if their bodies hold water component. Note that the composition of the binary planetary system is similar to that of the Earth-Moon system, and the composition of four binary satellite systems is also similar to that of the icy satellites of giant planets, this means that the fragments ejected from these binary planetary (satellite) systems may hold water composition.

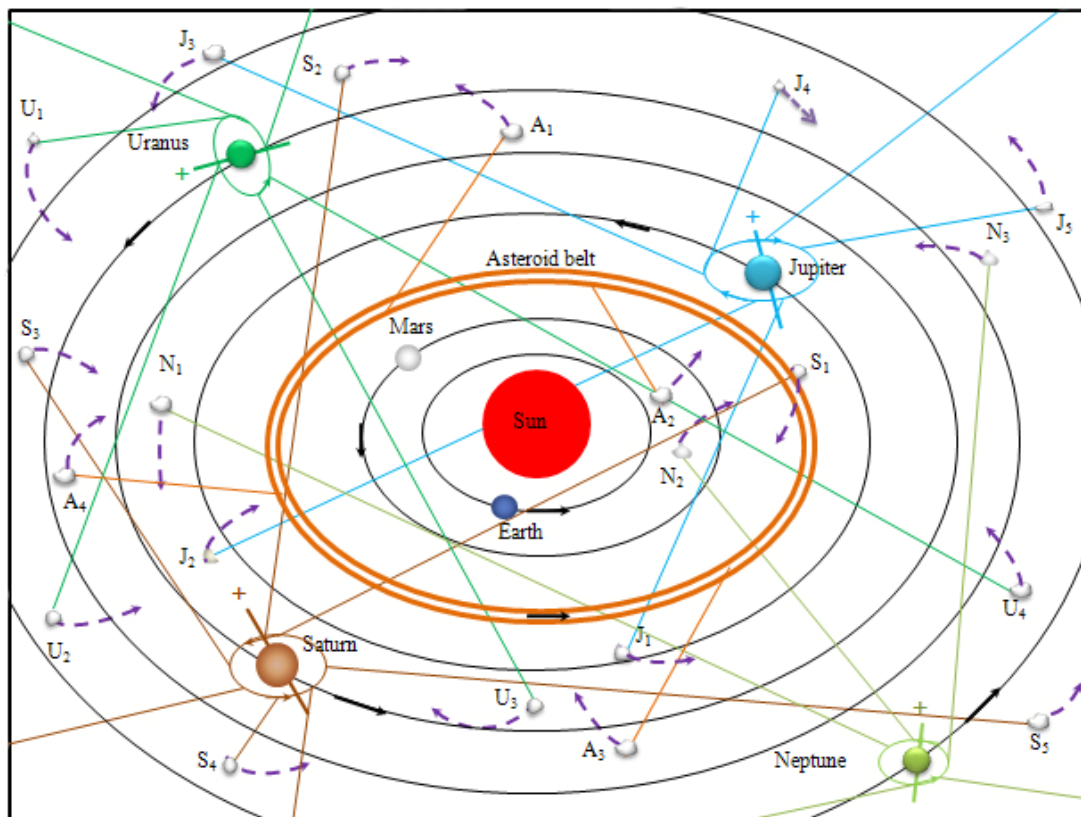


Figure 12: Motions of the fragments constrained by asteroid belt and four giant planets. Letter $A_{1,2,3}$, etc ($J_{1,2,3}$, etc, $S_{1,2,3}$, etc, $U_{1,2,3}$, etc, $N_{1,2,3}$, etc) respectively denote the fragments. Various colors of straight lines represent gravitations from asteroid belt and four planetary rings to these fragments. “+” denotes the north pole of the planet. Arrows denote the motional directions of fragments, planets, rings, and asteroid belt. Note that each fragment is running a parabolic trajectory around a barycenter that is located in asteroid belt (or giant planetary ring), but at the same time this motion is greatly influenced due to the motions of asteroid belt (giant planet) around the Sun.

As the distances of asteroid belt and Jupiter to the Sun are shorter than that of the Saturn, Uranus, and Neptune, this determines that asteroid belt and Jupiter may drag more fragments to approach the Sun to become comets than the Saturn, Uranus, and Neptune may do. As each fragment runs a parabolic trajectory around the barycenter that is located in asteroid belt (or planetary ring system), this determines that the comets dominated by asteroid belt and Jupiter should have shorter periods than those dominated by the Saturn, Uranus, and Neptune. Also because the orbital velocity of asteroid belt and Jupiter around the Sun is quicker than that of the Saturn, Uranus, and Neptune, the parabolic trajectories of the comets dominated by asteroid belt and Jupiter are easier to be dragged to fall on the elliptic than that of dominated by the Saturn, Uranus, and Neptune. In other words, short-period comets are likely to have less inclination (with respect to the elliptic) than long-period comets. Statistical results indicates that long period comets are generally on high-inclination orbits while short period ones are mostly on low-inclination prograde orbits (Duncan et al. 1988). But note that, because of a random ejection of fragments, the comets formed from these falling fragments will not have a prevailing direction in the sky.

Figure 12 reflects a relation that the value of $(\text{aphelion} - \text{perihelion})/2$ of a fragment is equal to the orbital radius of its owner (planet or asteroid belt) around the Sun. This may be an index to classify comets and centauries into different groups. Established literatures show that the perihelion and aphelion of Encke comet are 0.33 and 4.11 AU, respectively, the value of $(\text{aphelion} - \text{perihelion})/2$ is equal to 1.89 AU, which is roughly close to the orbital radius of main asteroid belt (average ~ 2.6 AU). The distance of Halley comet's orbit from the Sun is between 0.59 and 35.1 AU, the value of $(\text{aphelion} - \text{perihelion})/2$ is equal to 17.26 AU, which is roughly close to the orbital radius of Uranus (around 19.23 AU), Encke and Halley comets therefore may be considered to be dominated by asteroid belt and Uranus, respectively. But to ensure this classification, the established values of perihelion and aphelion must be reliable. According to Figure 12, we assumed that Encke comet runs a parabolic trajectory around a barycenter that is located in asteroid belt, the orbital radius and period of this barycenter around the Sun is 2.4 AU and 4.36 years, the orbital radius and period of Encke comet around this barycenter is 2.7 AU and 1.8 years, the inclination of this barycenter's orbit to the ecliptic is zero, the inclination of Encke comet's orbit to the ecliptic is 11.78 degrees. Observation shows that Encke comet once reached its closest approach to the Sun on 6 August 2010. We through JPL horizon system derive the

vector coordinate of Encke comet at this time: $x_{\text{Encke}} = -0.3149$ AU, $y_{\text{Encke}} = 0.1290$ AU, $z_{\text{Encke}} = -0.0037$ AU. As the barycenter's coordinate is unknown, it is necessary to use a mathematical method to work out. Geometrically speaking, if Encke comet is at perihelion, its position projection on the ecliptic must lie in the line between the Sun and this barycenter. We further assumed that the distance between the position projection and the barycenter is equal to the length of the orbital radius of Encke comet around this barycenter, therefore according to a geometry, the barycenter's coordinate is worked out to be $x_{\text{barycenter}} = 2.2189$ AU, $y_{\text{barycenter}} = -0.9150$ AU, $z_{\text{barycenter}} = 0.0000$ AU. Based on these coordinates and related parameters, the position of Encke comet at any time may be written as

$$x_t = 2.7 \times \sqrt{(1 - [\sin(\alpha + \frac{360}{1.8}t)]^2 \times [\sin \beta]^2)} \times \cos(\gamma + \frac{360}{1.8}t) + 2.4 \times \cos(\gamma + 180 + \frac{360}{4.36}t) \quad (4)$$

$$y_t = 2.7 \times \sqrt{(1 - [\sin(\alpha + \frac{360}{1.8}t)]^2 \times [\sin \beta]^2)} \times \sin(\gamma + \frac{360}{1.8}t) + 2.4 \times \sin(\gamma + 180 + \frac{360}{4.36}t) \quad (5)$$

$$z_t = 2.7 \times \sin(\alpha + \frac{360}{1.8}t) \times \sin \beta \quad (6)$$

Where t is time and its unit is year, α the initial angle of Encke comet to the intersection line that is between its orbit and the ecliptic, β the inclination of Encke comet orbit to the ecliptic that is equal to 11.78 degrees, γ the initial angle of its position projection to x axis.

The orbit of Encke comet is thus plotted (Fig.13). It can be found that Encke comet runs a very eccentric trajectory in space, repeatedly crosses the orbits of Mars and Earth, and even reaches the vicinity of Jupiter's orbit. It is also clear that, although Encke comet is specified an orbital period of 1.8 years around a barycenter that is located in asteroid belt, because of the motion of this barycenter around the Sun, the trajectory of Encke comet is seriously distorted in space. In the simulation the time interval between Encke comet's two closest approaches to the Sun is approximately 3 years, the aphelion and perihelion may reach 5.1 AU and 0.3 AU, respectively, the orbital velocity around the barycenter is around 44.69 km s^{-1} . It can also be found that the comet enters the inner solar system from one corner of the sky and then drops out, but next time it enters from another corner of the sky. This is consistent with the observation that Encke comet during past 9 apparitions does not have a prevailing direction when approaches the

Sun (Fig. 14). We expect that during a short period of time (from 2010-08-06 to 2017-12-20) the comet will experience two close approaches to the Earth, one close approach to the Mars, and one close approach to the Jupiter, more detail of these approaches is 0.27 AU from the Mars on 2010 November 26, 0.64 AU from the Jupiter on 2011 August 5, 0.57 AU from the Earth on 2013 July 13, and 0.36 AU from the Earth on 2016 November 15, the two closest approaches to the Sun are 0.58 AU on 2013 August 24 and 0.41 AU on 2016 September 27, respectively.

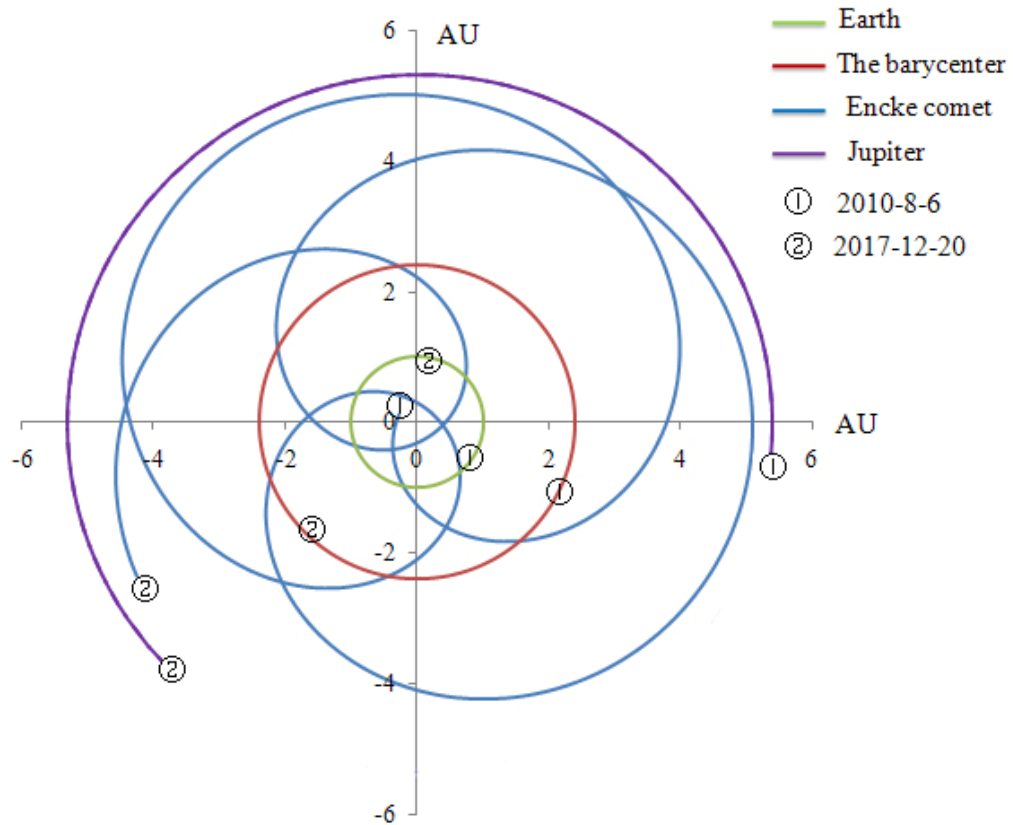


Figure 13: The orbit of Encke comet at the plane of the elliptic. The Sun is at the center. Time range is around 7 years. The coordinate origin is solar system barycenter (ssb). ① represents initial position of each body, while ② the final position of the body.

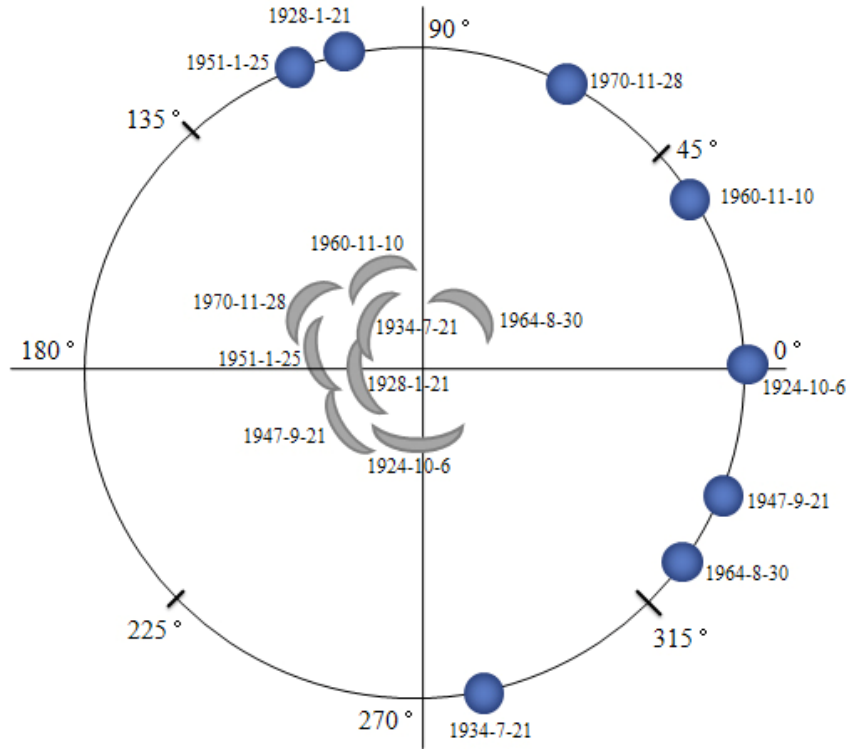


Figure 14: Relative positions between Encke comet's fan, Earth, and Sun during past 9 apparitions. The Sun is at the center. The data is from the work by Sekanina (1988). We firstly assumed that the Earth on 6 October 1924 is located at 0° , at this moment Encke comet's fan is at the east of the Sun, and from this time to 21 January 1928 the Earth orbits around the Sun totally 1202 days that is equivalent to 3 rotations + 105.55° , at this moment Encke comet's fan is at the west of the Sun. Similarly, the relative positions of Encke comet's fan, Sun, and the Earth during remaining 8 apparitions is determined.

In the past decades some small celestial bodies (Centaur) had been found. These objects are thought to be orbiting the Sun but crossing the orbits of one or more of the giant planets (Horner et al. 2008). This understanding, however, is not perfectly right, because if Centaur are orbiting around giant planets (Jupiter, Saturn, Uranus, for instance) and their orbit radius is large enough to cover the Sun's position, because of the motions of giant planets around the Sun, they will be brought to cross the orbits of giant planets, but this does not mean that they are orbiting around the Sun. According to the understanding of this paper, Centaur could be the fragments that were previously ejected from the disruptive collisions of the two bodies of binary satellite systems. We here determine that 2060 Chiron could be constrained by the Saturn on the assumptions that the

orbital radius, period, and inclination of it around Saturn is 17.9 AU, 40 years, and 6.93 degrees, respectively, and that the orbital radius, period, and inclination of Saturn around Sun is 9.55 AU, 29.46 years, and 2.48 degree. Reference to equations (4)(5)(6), we employ initial positions of related objects in 1996 from JPL's horizon system to run backward 20 years and forward 60 years, at the time the orbital radius of Chiron around Saturn is determined to be the distance between them. As shown in Figure 15, Chiron runs an orbit that is mainly located between the orbits of Saturn and Neptune, the aphelion and perihelion may reach 27.45 AU and 8.35 AU, respectively. The orbital velocity of Chiron around Saturn is worked out to be 13.33 km s^{-1} . It can be found that the orbit of Chiron between simulation and observation during the past 35 years are nearly consistent. The information from JPL Small-Body Database Browser shows that the aphelion, perihelion, orbital period, and orbital velocity of Chiron are 18.9 AU, 8.5AU, 50 years, and 7.75 km s^{-1} , respectively. It is necessary to note that Chiron was discovered in 1977 October, at the time it was thought to be near aphelion, this means that its real aphelion is unknown. As of 2012, the total observation for Chiron is not more than 35 years, this means that the real shape of a full orbit is also unknown. In contrast, the result of this simulation is competent. Astrometric record (<http://www.boulder.swri.edu/~buie/kbo/astrom/2060.html>) shows that the right ascension of Chiron varies from 2h 08'15" (1977 October) to 21h 05' 30" (2008 October), a circle of 24 h for Chiron orbiting celestial sphere thus corresponds to a time of approximately 39 years. We expect that in the following 45 years Chiron will experience one closest approach from the Uranus in 2027 January (around 1.0 AU), and its distance to Jupiter and Neptune will not be less than 13.5 AU.

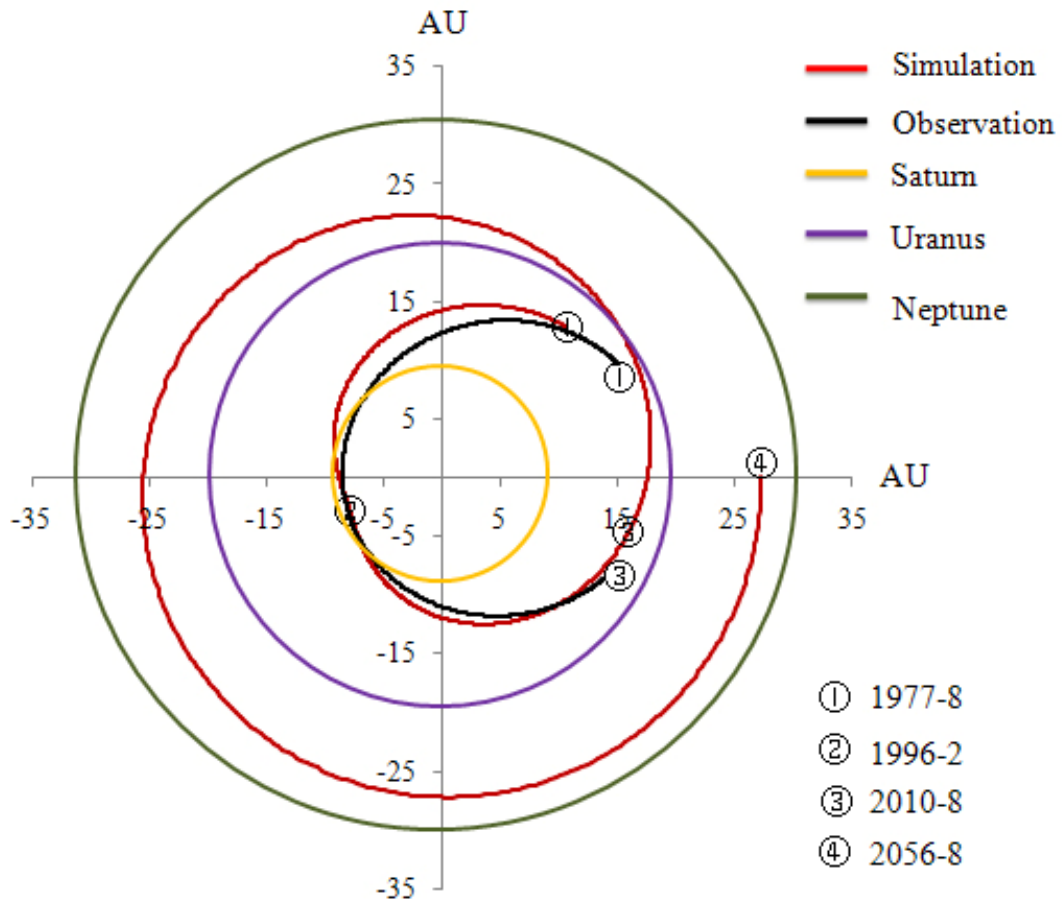


Figure 15: The orbit of 2060 Chiron at the plane of the elliptic. Time span is 80 years (1977~2056). Circle filled with number represent Chiron’s position at the corresponding time. The coordinate origin is solar system barycenter (ssb). Observation is from JPL’s horizon system.

4 Discussion

Celestial objects are evidently constrained by gravitational force to orbit, and the effect of gravitation is to drag object to mutually approach each other, thus with the passage of time the orbit of celestial object will be forced to decrease, and then the collision between the two bodies of a two-body system is destined. But this kind of orbital decrease in the solar system is absolutely not easy to be detected, the main reason is the Earth (observer) and other planets are located approximately at a plane, which makes radial astrometry extremely difficult. Comparatively speaking, the orbital decrease of stars and extrosolar planets is easy to be found if their orbital planes are approximately vertical to the line of sight. Another reason is that the amplitude of orbital decrease during a short time is too small to be detected. For instance, during a period of 100 years, the Earth has an orbital decrease of less than 4 km (according to the experienced

formula), the orbital decrease for other planets like the Mars, Jupiter, Saturn, and so are even small, while the Moon's orbital decrease is around 16 m. However, during a period of astronomical time, this kind of orbital decrease must be significant. Anyway, the observation of binary star systems, extrosolar planets, and the Phobos of Mars undoubtedly may confirm this existence of orbital decrease. In this paper, I use a geological record of coral fossil to deduce the amplitude of orbital decrease, many people must dispute that the variation of the number of days recorded in the coral fossil is the consequence of a slowing Earth's rotation. About this question, I here make an oral argumentation, while accurate analysis is left to be done in the future. For the Earth-Moon system, the two bodies are orbiting around a common center of their mass. This rotation may result in a centrifugal effect for them, but because of the pull of gravitation between them, the Earth's body is distorted into a prolate spheroid with major axis directed toward the Moon. The Earth is covered with a great deal of liquid water (around 71% of the Earth's surface), the heavier component may be thought to be immersed in the bottom of the water. The Earth's volume is conservative, this means that the heavier component due to a centrifugal effect will move away from the bottom of the water (away from the side of the Moon), this will extrude the water to flow toward the side of the Moon, by which the sea level that faces the Moon is thus boosted. Due to the Earth's rotation around its axis, the tide per day must undergo a rise and fall. On the other hand, the barycenter of the Earth-Moon system is orbiting around the Sun (actually around the barycenter of the third two-body system, reference to Figure 16) and this barycenter is geometrically located in the body of the Earth, the interaction of centrifugal effect and gravitation will further distort the Earth's body in the direction of line $3-O_1$. The orbit of the Moon relative to the ecliptic has a little inclination, this means that during a Moon's round (around 28 days) two kind of gravitations and centrifugal effects may together distort the Earth's body greatly, once the Sun (the barycenter of the third two-body system) and the Moon are approximately located at the same side of the Earth, sea level must be mutually boosted, if they are located at the opposite of the Earth, sea level must be mutually depressed, the tide per month thus undergoes an extreme height and low. However, the final result is determined by the interaction of a series of factors like sea water distribution, gravitation, and so on.

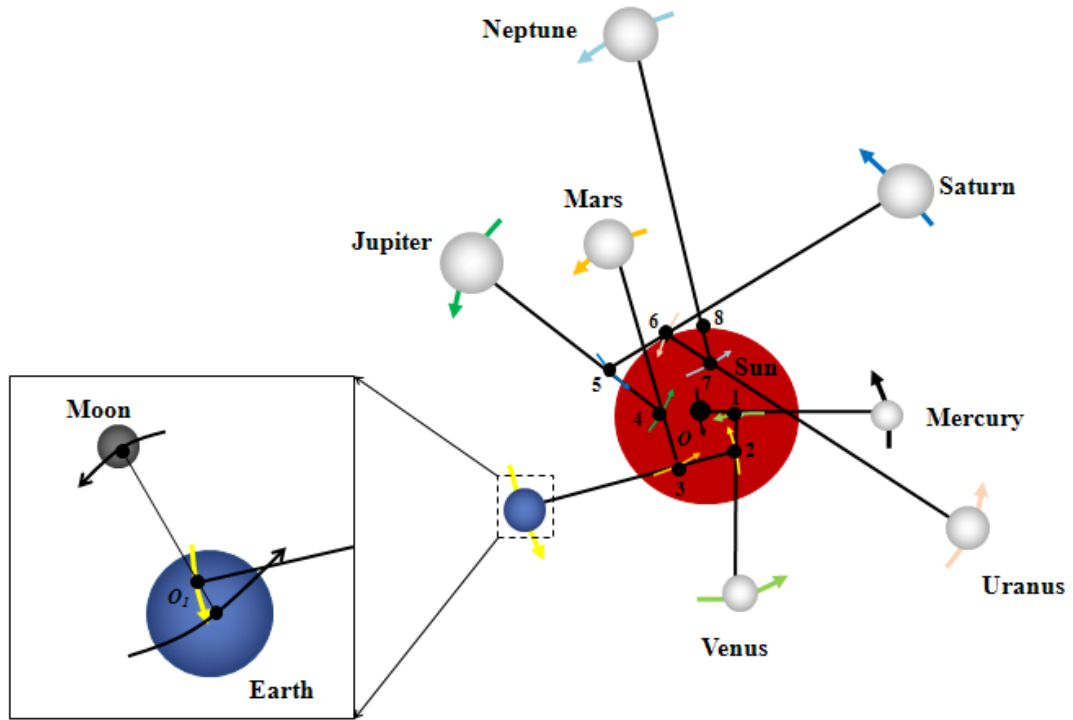


Figure 16: Configuration of the Sun and planets under a hierarchical two-body association. The Sun and Mercury form first two-body system, and at the same time the barycenter of this two-body system and Venus form second two-body system, etc. In each two-body system the two components are orbiting around the common center of their mass. Black dot 1, 2, 3, etc. respectively denote the barycenter of each two-body system, while O and O_1 represent the barycenters of the Sun and Earth-Moon system, respectively. Arrows represent the motional directions of each planet and two-body system. The diagram is from the work by Yang (2011). Note that asteroid belt is not included here.

In the solar system, the Earth has a satellite -the Moon. As of October 2009, more than 180 minor planets have been found to have moon (s) (reference to Johnston's Archive: Asteroids with Satellites). Each of four giant planets (Jupiter, Saturn, Uranus, and Neptune) generally holds a number of satellites, which makes it look like a small solar system. It is possible that some of these satellites in the past hold their own moons, but due to orbital shrinkage these moons had lost to the collision with their father satellites. Countless craters on the surfaces of planets and satellites suggest that they were severely bombarded after their formations but not before, this naturally requires some special events to responsible for. In recent years a number of irregular

moons have been found to orbit the Jovian planets, they form some groups and families that are similar to the asteroids in the main belt (Huebner 2000). It is undoubtedly certain that these irregular moons are the fragments that were ejected from the collisional events. As a result, it is not difficult to distinguish conventional moons from these irregular satellites. Conventional moons are often round (spherical) and massive, and their orbits are standard-circular and approximately parallel to planetary equatorial plane. For instance, Mimas, Enceladus, Tethys, Dione, Rhea, Titan, and Iapetus may be classified as the conventional moons of the Saturn, while the remaining should be the fragments of a previous binary satellite system; Io, Europa, Ganymede, and Callisto may be classified as conventional moons of the Jupiter, while the remaining should be the fragments of a previous binary satellite system; Miranda, Ariel, Umbriel, Titania, and Oberon may be classified as conventional moons of the Uranus, while the remaining should be the fragments of a previous binary satellite system; Triton may be classified as conventional moons of the Neptune, while the remaining should be the fragments of a previous binary satellite system. It is necessary to note that, as all irregular satellites are the fragments that were ejected from the collisions of the two bodies of the previous satellite systems, they must run parabolic trajectories around the barycenters that are located in the ring systems, this determines that their orbits (with respect to the planets) are highly eccentric and (with respect to planetary equatorial plane) are various inclinations. However, due to a successive hierarchical two-body drag, the inner irregular moons (close to the planet) are easier to form low-inclination orbits than the outer irregular moons. The low density of Saturn's small moons and their spectral characteristics similar to those of the main rings, closeness to the rings and rapid disruptive timescales have long suggested that their origin may be linked to the planet's icy rings (Jewitt et al. 2006; Nesvorny et al. 2003; Porco et al. 2007). Planetary rings are generally thought to be derived from the collisional fragmentations of a number of small bodies that once existed around the planet (Esposito 2002; Burns et al. 2001). The members of asteroid family (or group) are also thought to be the fragments produced by the disruption of a common parent body resulting from a catastrophic collision (Zappala et al. 2002). The work here supports these instinctive senses.

In the collision of the two bodies of the binary planetary system, the fragments ejected will be spherically distributed around the collisional origin. This means that the average orbital radius of the fragments around the Sun is approximately equal to the planetary system's orbital radius

around the Sun. We through JPL Small-Body Database Search Engine search for asteroids located at a range between Mars' and Jupiter's orbit ($1.52\text{AU} < R < 5.2\text{ AU}$). Around 536 818 asteroids are found and their average semi-major axis around the Sun and inclination with respect to the elliptic are worked out to be 2.67 AU and 8.30 degrees, respectively. As mentioned in section 3.1 of this paper, at present the barycenter of initial binary planetary system is most likely to be located at the inner edge of main belt, the main belt is at a distance of $2.15 \sim 3.3\text{ AU}$ from the Sun, if the orbital radius is $R_o = 2.15\text{ AU}$, this will correspond to an orbital period of 3.9 years. These should be the constraints of the barycenter (point O) of initial binary planetary system orbiting the Sun at present.

If such a smashing collision had occurred for the proposed binary planetary system in the past, a natural aftermath is that a large number of fragments would be ejected from the collisional origin towards all around (reference to Figure 1), and therefore can bombard the objects they encounter in the travel, and thereby leave craters and scrapes on the surfaces of these objects. In general, the nearer the objects are from the collisional source, the more the objects can encounter bombardment from the fragments. As shown in Figure 17, when the fragments from the collisional origin are ejected, the Mars and Earth in their orbits can inevitably be bombarded by some of the ejecting fragments. As the Mars is close to the collisional source more than the Earth, the Mars and its satellites can naturally receive more bombardment than the Earth and Moon can do. In particular, the synchronous rotation of the Moon around the Earth can get its far side receive more bombardment than the near side. As stated previously in this paper, the ejected fragments under the effect of hierarchical two-body confinement can be dragged to fall on a circular belt, also because the Moon is a sphere and its orbit has an inclination of 5.15 degrees to the elliptic, this determines that the Moon in motion can repeatedly run through part of the fragment belt. In the course of penetration, the south and north poles of the Moon can inevitably collide with the fragments to leave heavy craters (Fig.18). We must remember that, because of the existence of orbital decrease, the Mars and Earth in the past should be more near to asteroid belt than in the present. This means that both of them might have encountered more bombardment in the past than in the present. From Figure 17, we conclude, the satellites of the Mars (Deimos and Phobos) might had hold perfect spherical shape like the Earth's satellite- the Moon, but subsequently they were severely bombarded by the fragments and thereby left disabled structures, a heavy bombardment

may also destroy the Mars's shroud if it is surrounded by thick atmosphere like what on the Earth, by which the climate system is seriously disturbed, for instance, water composition may escape toward outer space, and then wet climatic surroundings on the Mars disappears.

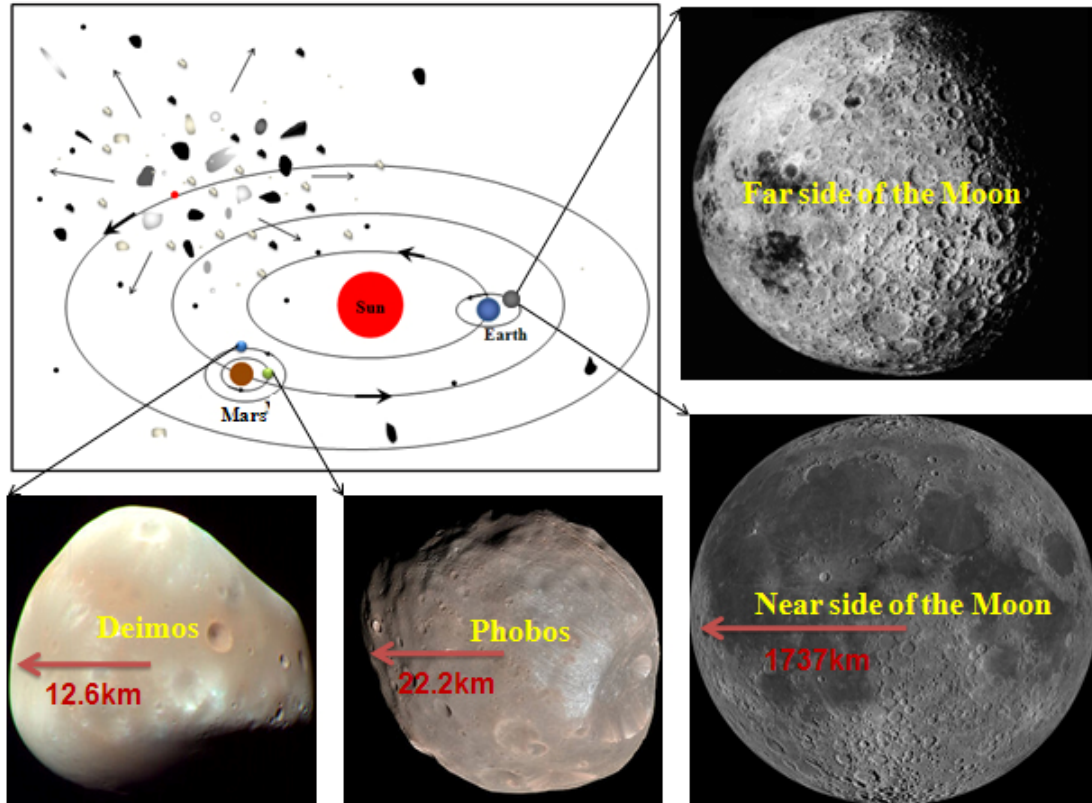


Figure 17: Ejecting fragments inward bombard planets and their satellites to form various craters. Red dot in the model diagram represents the barycenter of the proposed planetary system. Images of Deimos, Phobos, far side of the Moon, and near side of the Moon are by the courtesy of NASA.

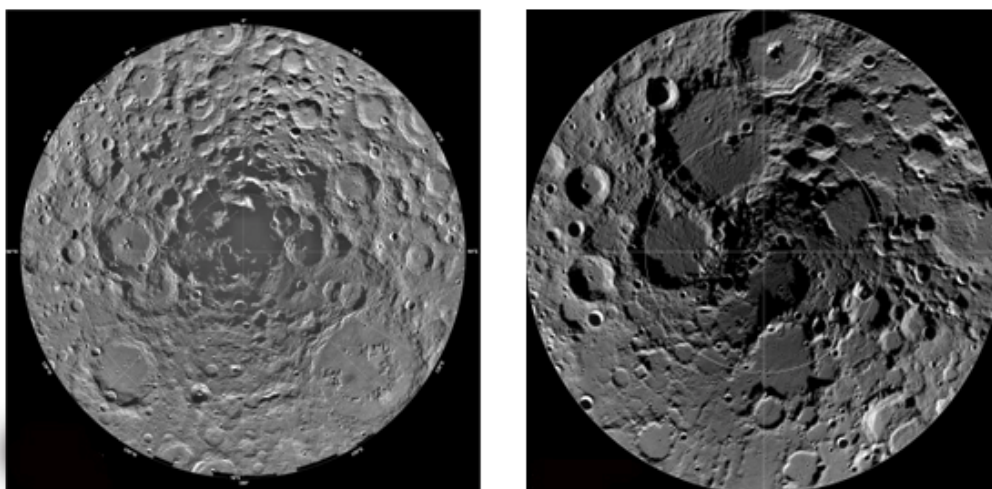


Figure 18: South (left) and North (right) Poles of the Moon. Images are by the courtesy of

A latest analysis of dust particles from near-Earth asteroid 25 143 Itokawa shows that the asteroid is likely to be made of reassembled pieces of the interior portions of a once larger asteroid (Nakamura et al. 2011). This means that larger asteroids might have been further shattered into smaller asteroids. The impact crater record of the terrestrial planets and the Moon confirms an inner solar system impact cataclysm occurred 3.9 Gy ago, and identifies the main asteroid belt as the source of the impactors (Strom et al. 2005). The heavily cratered surfaces on Ganymede and Callisto discovered by Voyager 1 confirms another kind of bombardment occurred in the outer solar system (Strom et al. 1981). Possible causes proposed for these bombardments include gas giant migration (Gomes et al. 2005) and Late Uranus/Neptune formation (Levison et al. 2001). However, the story of gas giant migration has two uncertainties, the first is it assumed a rich trans-Neptunian belt to firstly interact with giant planets, but so far no evidence can support the existence of this trans-Neptunian belt, the second is it cannot account for the difference of crater distribution, for instance, on the Moon's surface there are more craters on the far side than on the near side, most importantly, the craters on the south and north poles appear to be more serious than on the near and far sides. The proposal of late Uranus/Neptune formation has not yet obtained support from numerical simulation. In recent years NASA John Chambers and Jack Lissauer proposed a fifth planet (V) that exists between Mars and the asteroid belt to increase crater rate, but Planet V and its disruption are unclear, too. The comparison of cratering record from Mercury to Uranus shows that the solar system cratering record cannot be explained by a single family of objects in heliocentric orbits, e.g., comets (Strom 1987). All these problems strongly require a more compelling model to account for. In a private communication with professor Robert G. Strom, he stated that the younger population of crater has been accumulating from the end of the period of Late Heavy Bombardment about 3.8 -3.7 ba up to the present time. In this present paper we totally propose 5 collisional scenarios: one occurred in the inner solar system around 3.9 ba that yielded a large number of fragments to create the old population of craters (the Late Heavy Bombardment), other four independently occurred in the outer solar system after the Late Heavy Bombardment (later than 3.8 ba) that yielded a lot of fragments to create the younger population of craters, but as all fragments are running parabolic trajectories around the barycenters in asteroid

belt and planetary rings, they will gradually return to asteroid belt and planetary rings, in this falling process an accumulating population of craters may be formed on the surfaces of planets and satellites. The collision of comet Shoemaker-Levy and Jupiter may be such a case.

A large number of meteorites in the past have been found on the Earth. The majority of the meteorites are chondrites, they are composed mostly of silicate minerals that appear to have been melted while they were free-floating objects in space. Even some types of chondrites contain small amounts of organic matter (Ceplecha et al. 1961). But the scenario that accounts for the origin of meteorite remains uncertain. The majority of meteorites are believed to come from asteroid belt, some are thought to come from the Moon and the Mars due to the dispersion of impactors. Indeed, the chemical composition of the majority of meteorites is similar to that of the asteroids in the belt (plentiful carbonaceous and silicate material but less metallic material, for instance), but this needs a mechanism to explain how meteorites transport from asteroid belt to the Earth. Carrying meteorites from the Moon and Mars to the Earth appears to be extremely difficult, because it needs to consider the connection of a series of transporting events. Moreover, meteorites have been found in different places, NASA's Opportunity Rover in 2005 captured an iron meteorite on the Mars. The collision of the two bodies of a previous binary planetary system may create such a condition for fragments to travel and land on the surfaces of planets and satellites and further become meteorites. In the collision some melting materials (including rock and iron) in the bodies of the binary planetary system may be released and recrystallized, while some organic matter may be sealed in the voids of fragments.

The observation of comet has a history of more than thousands of years, but its origin and dynamics long-term keep disputed. The main reason is that their appearances are very short-lived and can be seen just when close to the Sun, most of the time, their orbits are unclear. Oort cloud hypothesis and Kuiper belt hypothesis undoubtedly fail in several aspects. At least, a flat solar system anyway cannot support a spherical distribution of icy materials, and transporting icy materials from Kuiper belt to inner solar system is nothing but a guess. According to Figure 3, we can infer that the final orbital velocity of a fragment is between $V_1+V_2 \sim V_1-V_2$, regardless of the effect of gravitation, this means that the comet's orbital velocity may be various, namely some of the comets may hold very rapid speed in space. A rapid comet naturally requires a strong force to control, reference to Figure 12 and 16, the Sun and all planets together are indirectly responsible

for the motions of these fragments by means of the barycenters of a series of hierarchical two-body systems. Evidently, the fragments controlled by asteroid belt and giant planets may run cross the orbits of planets if their orbital radius is large enough. Once these fragments are close to the Sun enough, volatile impression is natural. Most of comets are composed of water ice, rock, dust, and frozen gases (Poulet et al. 2003), planetary ring also consists of mainly water ice and dust. As of 2008, three centaurs such as 2060 Chiron, 60558 Echeclus, and 166P/NEAT have been found to display cometary coma (Coradini et al. 2009). This similarity indicates that the origin of planetary ring and comet (centaur) could be related. The comet's fan, the Sun, and the comet's owner (asteroid belt or giant planet) must lie on a straight line, this may be an index to classify comet.

Clearly, the observation of asteroid family and planetary ring demands explanation far more than established knowledge can do. For instance, the members of asteroid family appear to be wholly froze in proper orbital elements space (Zappal'a et al. 1996), this stability is nearly constant on a 10^7 - 10^8 years' time scale (Milani and Farinella 1994). The family's members are spatially separated, this means some of the members are near to the side of the Sun. If Newton's gravity is applicable, the Sun's gravitation will require each member in the family to make Keplerian motion, the longitudinal differential motion between the members will finally terminate the family. In addition, the mutual attraction between these members will lead them to centralize and thereby disturbs the constant proper orbital elements. Self-gravity was proposed to keep the stability of asteroid family. This consideration is questionable because the gravitation of the Sun to a family's member is far larger than the total gravitation of all other members to this member, this also requires each family's member to make Keplerian motion. Flora family has a population of more than 590 members that cover a radial width of ~ 0.2 AU, and its largest member is Flora 8 that accounts for 80% the mass of the family. If the longitudinal width of these members is assumed to be 0.2 AU, the average distance between any two adjacent members in the family is around 10 000 km. The mass of Flora 8 is 4.3×10^{18} kg (Michalak, G 2001), the family's mass is thus worked out to be 5.4×10^{18} kg. If all mass of the family is ideally centralized at the position of a member, the Sun's gravitation to this member's neighbor will be around 460 times that of the family to the neighbor. In practice, the largest two members Flora 8 and 43 Ariadne are located near the edge of the family. This unusual mass distribution within the family is evidently against

Newton's gravity. For instance, the majority of planetary rings in appearance are flat. This flattening is often explained as the collisions of a swarm of particles that dissipates mechanical energy, while angular momentum of the system is conservative. This consideration is very questionable, because different spectral characteristics' rings in the Saturn's ring system are parallel to one another and there are also divisions (gaps) between them, the collision between particles can inevitably lead them to randomly eject (at least in both the radial and longitudinal directions), any mixture of particles will not allow the existence of the distribution of parallel, separated, different material rings. The Saturn's C ring reflects this kind of feature well. In contrast, the collisional scenarios of the two bodies of binary planetary (satellite) system proposed in this paper may clear out these questions. The hierarchical two-body gravitation still follows an inverse-square law, but its expression is not direct but indirect. The object's mass and gravitational constant we use in this paper are from the estimation of Newton's gravity, but these approximate values may be utilized if a relative calculation is operated. The work in this paper provides a starting point to comprehensively consider the origin of asteroid belt, planetary ring, and comets, along with craters and meteorites, future work in both observation and numerical simulation may strengthen the expectation of this model.

Acknowledgments I thank my family for their great understanding and support in doing this work.

References

- E. A. Roche, Acad. Sci. Lett. Montpellier. Mem. Section Sci. **1**, 243 (1847)
- J. B. Pollack , A. S. Grossman, R. Moore, H. C. Jr. Graboske, Icarus **29**, 35 (1976)
- S. Charnoz, A. Morbidelli, L. Dones, J. Salmon, Icarus **199**, 413 (2009)
- L.Dones, Icarus **92**, 194 (1991)
- R. M. Canup, Nature **000**,1 (2010)
- W. Herschel, Philosophical Transactions of the Royal Society of London **97**, 271(1807)
- J.-M. Petit, A. Morbidelli, J. Chambers, Icarus **153**, 338 (2001)
- J. H. Oort, Bull. Astron. Inst. Neth.**11**, 91 (1950)
- G. P.Kuiper, In Astrophysics: A Tropical Symposium, edited by J. A. Hynek. Mcgraw-Hill, New

- York, 357 (1951)
- S. Charnoz, J. Salmon and A. Crida, *Nature* **465**, 752 (2010)
- J. A. Burns, D. P. Hamilton, M. R. Showalter, B. A. S. Gustafson, S. F. Dermott and H. Fechtig
(Berlin: Springer) pp 641 (2001)
- P. Goldreich, S. Tremaine, *Nature* **277**, 97 (1979)
- C. C. Porco, P. Goldreich, *AJ.* **93**, 724 (1987)
- B. A. Smith, *et al.*, *Science* **233** (4759), 97 (1986)
- E. D. Miner, R. R. Wessen, J. N. Jeffrey, *Planetary Ring System*. Springer Praxis Books (2007)
- B. A. Smith, *et al.*, *Science* **246** (4936), 1422(1989)
- H. Salo and J. Hänninen, *Science* **282** (5391): 1102(1998)
- C. Dumas, *et al.*, *Nature* **400** (6746), 733(1999)
- B. Sicardy, *et al.*, *Nature* **400** (6746), 731(1999)
- F. Namouni & C. Porco, *Nature* **417**, 45(2002)
- B. Sicardy & S. Renner, *Bull. Am. Astron. Soc.* **35**, 929(2003)
- S. Renner & B. Sicardy, *Celestial Mechanics* **88**, 397 (2004)
- M. M. Woolfson, *Q. J. R. Astr. Soc.* **34**, 1(1993)
- N. Taishi, N. Yushitsugu, *ApJ.* **421**, 640 (1994)
- A. N. Youdin, F. N. Shu, *ApJ.* **580**, 494 (2002)
- H. H. Klahr, P. Bodenheimer, *ApJ.* **582**, 869 (2003)
- S. Inaba, G. W. Wetherill, M. Ikoma, *Icarus* **166**, 46 (2003)
- G. Wurchterl, *Kluwer Academic Publishers* (2004), pp 67–96
- M. Duncan, T. Quinn, S. Tremaine, *ApJ, Part 2 -Letters* **328**, L69 (1988)
- H. H. Hsieh, D. Jewitt, *Science* **312**, 61(2006)
- L. W. Esposito, *Reports On Progress In Physics* **65**, 1741 (2002)
- I. d. Pater, H. B. Hammel, S. G. Gibbard, M. R. Showalter, *Science* **312**, 92 (2006)
- R. G. Strom, *et. al.*, *Science* **309**, 1847 (2005)
- R. G. Strom, *et. al.*, *Journal of Geophysical Research* **86**, 8659 (1981)
- R. L. Kelley, *et. al.*, *ApJ*, **268**, 790(1983)
- A. Levine, *et. al.*, *ApJ*, **410**, 328(1993)
- J. M. Weisberg, J. H. Taylor, *Binary Radio Pulsars ASP Conference Series, Vol. TBD, 2004 eds.*

- F.A. Rasio & I.H. Stairs
- C. Terquem and J. C. B. Papaloizou, *ApJ*, **654**, 1110(2007)
- A. Brunini & R. G. Cionco, *Icarus* **177**, 264(2005)
- S. N. Raymond, R. Barnes, & A. M. Mandell, *MNRAS* **384**, 663(2008)
- D. Charbonneau, *et al.*, *Nature* **462**, 891(2009)
- S. Clark, "Flights to Phobos" in *New Scientist* magazine, 30th January 2010
- K. Hirayama, *AJ*. **31**, 185 (1918)
- C. D. Murray, *et al.*, *Nature* **453**, 739 (2008)
- H. Hammel, Springer Praxis Books (2006), pp251-265
- Y. F. Yang, Proceedings of the 18th annual conference of the NPA, College Park, Maryland University, USA, Vol.8, 712 (2011). viXra:1010.0042
- E. F., Tedesco, F. -X., *Desert, AJ*, **123** (4), 2070(2002).
- S. G. Love, D. E. Brownlee, *AJ*.**104** (6), 2236 (1992)
- Y. Funato, *et al.*, *Nature* **427**, 518 (2004)
- D. D. Durda, *et al.*, *Icarus* **170**, 243 (2004)
- S. J. Weidenschilling, *Icarus* **160**, 212 (2002)
- P. Goldreich, Y. Lithwick, & R. Sari, *Nature* **420**, 643(2002)
- S. A. Astakhov, E. A. Lee, & D. Farrelly, *Mon.Not. R. Astron. Soc.* **360**, 401(2005)
- R. M. Canup, *Science* **307**, 546(2005)
- J. L. Margot, *et al.*, *Science* **296**, 1445(2002)
- W. J. Merline, *et al.*, *Asteroids III* 289 (Univ. Arizona Press, Tucson, 2002)
- D. C. Stephens, & K. S. Noll, *AJ*. **131**,1142 (2006)
- L. W. Esposito, *et al.*, *Icarus* **194**, 278(2008)
- M. Duncan, T. Quinn, T. Scott, *ApJ*. **328**, L69 (1988)
- Z. Sekanina, *AJ*. **95**, 911(1988).
- J. Horner, N.W. Evans, *Mon. Not. R. Astron. Soc.* **000**,1 (2008)
- W. F. Huebner, *Earth, Moon, and Planets.* **89**,179 (2000)
- D. C. Jewitt, A. Delsanti, *Solar System Update : Topical and Timely Reviews in Solar System Sciences.* Springer-Praxis Ed (2006)
- D. Nesvorny, J. L. A. Alvarellos, L. Dones, H. Feverson, *AJ*. **126**, 298 (2003)

- C. C. Porco, *et al.*, *Science* **318**, 1602 (2007)
- V. Zappalà, A. Cellino, A. Dell'Oro, P. Paolicchi, In *Asteroids III* (W. F. Bottke Jr. et al., eds.),
this volume. Univ. of Arizona, Tucson (2002)
- T. Nakamura, *et al.*, *Nature* **333**, 1113 (2011)
- R. Gomes, H. F. Levison, K. Tsiganis, A. Morbidelli, *Nature* **435**, 466 (2005)
- H. F. Levison, *et al.*, *Icarus* **151**, 286 (2001)
- R. G. Strom, *Icarus* **70**, 517 (1987)
- Z. Ceplecha, *Bull. Astron. Inst. Czechoslovakia* **12**, 21(1961)
- F. Poulet, *et al.*, *Astron. Astrophys.* **412**, 305 (2003)
- A. Coradini, *et al.*, *Earth Moon Planets* **105**, 289 (2009)
- V. Zappala, *et al.*, *Icarus* **124**, 156(1996)
- A. Milani and P. Farinella, *Nature* **370**, 40 (1994)
- G. Michalak, *Astronomy & Astrophysics* **374** (2),703 (2001)